



**HAL**  
open science

## Shifting Fc $\gamma$ RIIA-ITAM from activation to inhibitory configuration ameliorates arthritis.

Sanae Ben Mkaddem, Gilles Hayem, Friederike Jönsson, Elisabetta Rossato, Erwan Boedec, Tarek Boussetta, Jamel El Benna, Pierre Launay, Jean-Michel Goujon, Marc Benhamou, et al.

### ► To cite this version:

Sanae Ben Mkaddem, Gilles Hayem, Friederike Jönsson, Elisabetta Rossato, Erwan Boedec, et al.. Shifting Fc $\gamma$ RIIA-ITAM from activation to inhibitory configuration ameliorates arthritis.. Journal of Clinical Investigation, 2014, 124 (9), pp.3945-3959. 10.1172/JCI74572 . pasteur-02512366

**HAL Id: pasteur-02512366**

**<https://pasteur.hal.science/pasteur-02512366v1>**

Submitted on 19 Mar 2020

**HAL** is a multi-disciplinary open access archive for the deposit and dissemination of scientific research documents, whether they are published or not. The documents may come from teaching and research institutions in France or abroad, or from public or private research centers.

L'archive ouverte pluridisciplinaire **HAL**, est destinée au dépôt et à la diffusion de documents scientifiques de niveau recherche, publiés ou non, émanant des établissements d'enseignement et de recherche français ou étrangers, des laboratoires publics ou privés.



Distributed under a Creative Commons Attribution 4.0 International License

# Shifting FcγRIIA-ITAM from activation to inhibitory configuration ameliorates arthritis

Sanae Ben Mkaddem, ... , Pierre Bruhns, Renato C. Monteiro

*J Clin Invest.* 2014;124(9):3945-3959. <https://doi.org/10.1172/JCI74572>.

Research Article

Inflammation

Rheumatoid arthritis–associated (RA-associated) inflammation is mediated through the interaction between RA IgG immune complexes and IgG Fc receptors on immune cells. Polymorphisms within the gene encoding the human IgG Fc receptor IIA (hFcγRIIA) are associated with an increased risk of developing RA. Within the hFcγRIIA intracytoplasmic domain, there are 2 conserved tyrosine residues arranged in a noncanonical immunoreceptor tyrosine–based activation motif (ITAM). Here, we reveal that inhibitory engagement of the hFcγRIIA ITAM either with anti-hFcγRII F(ab')<sub>2</sub> fragments or intravenous hIgG (IVIg) ameliorates RA-associated inflammation, and this effect was characteristic of previously described inhibitory ITAM (ITAMi) signaling for hFcαRI and hFcγRIIIA, but only involves a single tyrosine. In hFcγRIIA-expressing mice, arthritis induction was inhibited following hFcγRIIA engagement. Moreover, hFcγRIIA ITAMi-signaling reduced ROS and inflammatory cytokine production through inhibition of guanine nucleotide exchange factor VAV-1 and IL-1 receptor–associated kinase 1 (IRAK-1), respectively. ITAMi signaling was mediated by tyrosine 304 (Y304) within the hFcγRIIA ITAM, which was required for recruitment of tyrosine kinase SYK and tyrosine phosphatase SHP-1. Anti-hFcγRII F(ab')<sub>2</sub> treatment of inflammatory synovial cells from RA patients inhibited ROS production through induction of ITAMi signaling. These data suggest that shifting constitutive hFcγRIIA-mediated activation to ITAMi signaling could ameliorate RA-associated inflammation.

Find the latest version:

<https://jci.me/74572/pdf>



# Shifting Fc $\gamma$ RIIA-ITAM from activation to inhibitory configuration ameliorates arthritis

Sanae Ben Mkaddem,<sup>1,2,3,4</sup> Gilles Hayem,<sup>5</sup> Friederike Jönsson,<sup>6,7</sup> Elisabetta Rossato,<sup>1,2,3,4</sup> Erwan Boedec,<sup>1,2,3,4</sup> Tarek Boussetta,<sup>1,2,3,4</sup> Jamel El Benna,<sup>1,2,3,4</sup> Pierre Launay,<sup>1,2,3,4</sup> Jean-Michel Goujon,<sup>8</sup> Marc Benhamou,<sup>1,2,3,4</sup> Pierre Bruhns,<sup>6,7</sup> and Renato C. Monteiro<sup>1,2,3,4</sup>

<sup>1</sup>INSERM, U1149, Centre de Recherche Sur l'Inflammation, Paris, France. <sup>2</sup>CNRS ERL8252 and <sup>3</sup>Université Paris Diderot, Sorbonne Paris Cité, Faculté de Médecine, Site Xavier Bichat, Paris, France.

<sup>4</sup>Laboratoire d'Excellence Inflammex and <sup>5</sup>Department de Rhumatologie, Assistance Publique-Hôpitaux de Paris, Université Paris Diderot, Sorbonne Paris Cité, Hôpital Bichat Claude Bernard,

Paris, France. <sup>6</sup>Institut Pasteur, Département d'Immunologie, Laboratoire Anticorps en Thérapie et Pathologie, Paris, France. <sup>7</sup>INSERM, U760, Paris, France. <sup>8</sup>Service d'Anatomie et Cytologie

Pathologiques, Centre Hospitalier Universitaire de Poitiers, Université de Poitiers, Poitiers, France.

**Rheumatoid arthritis-associated (RA-associated) inflammation is mediated through the interaction between RA IgG immune complexes and IgG Fc receptors on immune cells. Polymorphisms within the gene encoding the human IgG Fc receptor IIA (hFc $\gamma$ RIIA) are associated with an increased risk of developing RA. Within the hFc $\gamma$ RIIA intracytoplasmic domain, there are 2 conserved tyrosine residues arranged in a noncanonical immunoreceptor tyrosine-based activation motif (ITAM). Here, we reveal that inhibitory engagement of the hFc $\gamma$ RIIA ITAM either with anti-hFc $\gamma$ RII F(ab')<sub>2</sub> fragments or intravenous hIgG (IVIg) ameliorates RA-associated inflammation, and this effect was characteristic of previously described inhibitory ITAM (ITAMi) signaling for hFc $\alpha$ RI and hFc $\gamma$ RIIIA, but only involves a single tyrosine. In hFc $\gamma$ RIIA-expressing mice, arthritis induction was inhibited following hFc $\gamma$ RIIA engagement. Moreover, hFc $\gamma$ RIIA ITAMi-signaling reduced ROS and inflammatory cytokine production through inhibition of guanine nucleotide exchange factor VAV-1 and IL-1 receptor-associated kinase 1 (IRAK-1), respectively. ITAMi signaling was mediated by tyrosine 304 (Y304) within the hFc $\gamma$ RIIA ITAM, which was required for recruitment of tyrosine kinase SYK and tyrosine phosphatase SHP-1. Anti-hFc $\gamma$ RII F(ab')<sub>2</sub> treatment of inflammatory synovial cells from RA patients inhibited ROS production through induction of ITAMi signaling. These data suggest that shifting constitutive hFc $\gamma$ RIIA-mediated activation to ITAMi signaling could ameliorate RA-associated inflammation.**

## Introduction

Rheumatoid arthritis (RA) is a chronic autoimmune inflammatory disease. Neutrophils, lymphocytes, mast cells, macrophages, synovial tissue cells, and platelet microparticles present in the inflamed synovium have been implicated in RA pathophysiology (1, 2). Circulating autoantibodies are present in a majority of RA patients, and joint tissue is frequently covered with immune complexes (ICs) (3, 4) mainly composed of rheumatoid factors and ICs formed of anti-cyclic citrullinated peptide (anti-CCP) IgG antibodies and CCP.

RA IgG ICs bind to IgG Fc receptors (FcRs) that play an essential role in disease progression. Neutrophils and monocytes are FcR-bearing cells that contribute to joint inflammation via the release of inflammatory mediators that increase vascular permeability and promote further immune cell recruitment (1). There are 3 main classes of human FcRs (hFcRs): hFc $\gamma$ RI (CD64), hFc $\gamma$ RII (CD32), and hFc $\gamma$ RIII (CD16). They differ in function, cell distribution, and IgG-binding capacity (5). Three isoforms of hFc $\gamma$ RII have been identified: hFc $\gamma$ RIIA, hFc $\gamma$ RIIB, and hFc $\gamma$ RIIC. Among them, hFc $\gamma$ RIIA is a potent activator of inflammation. hFc $\gamma$ RIIA is expressed by all myeloid cells and platelets. hFc $\gamma$ RIIA possesses an immunoreceptor tyrosine-based activation motif (ITAM) in

its intracytoplasmic domain and, in contrast with hFc $\gamma$ RI and hFc $\gamma$ RIIIA, is not associated with the ITAM-bearing subunit FcR $\gamma$  (6–8). hFc $\gamma$ RIIA is a low-affinity receptor that interacts with all 4 human IgG subclasses (9) as well as mouse IgG1, IgG2a, and IgG2b (10). There is no Fc $\gamma$ RIIA homolog in the mouse (5). Cross-linking of hFc $\gamma$ RIIA by IgG ICs results in the phosphorylation of ITAM tyrosine residues, followed by recruitment and activation of the tyrosine kinase Syk. This leads to calcium mobilization, activation of MAPK pathways, activation of NF- $\kappa$ B, and inflammatory cell activation (11). Two codominantly expressed alleles of hFc $\gamma$ RIIA differ by an arginine or a histidine at amino acid position 131 and by their affinity for hIgG2. The hFc $\gamma$ RIIA-H131 variant is the only IgG receptor that efficiently binds human IgG2 (12). The hFc $\gamma$ RIIA-R131 variant is associated with an increased risk of developing RA (13). Transgenic expression of hFc $\gamma$ RIIA-R131 on neutrophils and monocytes of mice lacking endogenous activating FcR (due to ablation of the FcR $\gamma$  chain gene that is required for mFc $\gamma$ RI, mFc $\gamma$ RIII, mFc $\gamma$ RIV, and mFc $\epsilon$ RI expression) restores susceptibility to autoimmune diseases and passive proinflammatory reactions (14). Most interestingly, hFc $\gamma$ RIIA-R131 transgenic mice are highly susceptible to both collagen-induced arthritis (CIA) and collagen antibody-induced arthritis (CAIA) and spontaneously develop multisystem autoimmune diseases (15).

Fc $\gamma$ RIIB, which is conserved in mice and humans, is a single-chain inhibitory FcR. Fc $\gamma$ RIIB contains a tyrosine-based inhibition motif (ITIM) in its cytoplasmic region (16). Inhibition is

**Authorship note:** Gilles Hayem and Friederike Jönsson contributed equally to this work.

**Conflict of interest:** The authors have declared that no conflict of interest exists.

**Submitted:** December 3, 2013; **Accepted:** May 30, 2014.

**Reference information:** *J Clin Invest.* 2014;124(9):3945–3959. doi:10.1172/JCI74572.

dependent on the isotype of IgG and on Fc $\gamma$ RIIB expression levels. The classic concept of the functional polarity of ITIM and ITAM motifs has been recently reevaluated. Several studies have demonstrated that ITAM can also initiate inhibitory signaling toward heterologous receptors. This active inhibitory signaling by ITAM-bearing receptors is called inhibitory ITAM (ITAMi) (17–19). Thus, the human IgA receptor hFc $\alpha$ RI, which is associated with FcR $\gamma$ , acts as a bifunctional module that, depending on the type of interaction with its ligand, induces either activating or inhibitory cell signaling (18). Although multivalent crosslinking of hFc $\alpha$ RI with IgA ICs induced proinflammatory signaling (20), monovalent targeting of hFc $\alpha$ RI with monomeric IgA (or Fab anti-Fc $\alpha$ RI) in the absence of antigen can trigger inhibitory signals toward a whole array of cellular functions such as IgG-dependent phagocytosis and TLR- or cytokine-mediated responses (21, 22). Strikingly, monovalent targeting of hFc $\alpha$ RI (termed “ITAMi configuration”) induces weak ITAM phosphorylation of the FcR $\gamma$  subunit and transient recruitment of Syk followed by stable recruitment of the tyrosine phosphatase SHP-1, whereas multivalent aggregation of the receptor promotes strong ITAM phosphorylation with stable Syk recruitment. Recruitment of SHP-1 in the ITAMi configuration promotes the actin depolymerization-dependent “trapping” of hFc $\alpha$ RI and of the targeted activating receptors within the same lipid rafts, followed by the appearance of intracellular clusters called inhibisomes (23). Recently, we demonstrated that hFc $\gamma$ RIIIA (CD16A), which is also associated with the common FcR $\gamma$  subunit, was similarly able to induce ITAMi signaling following interaction with hIgG1, i.e. hIgG (IVIg), or F(ab) $_2$  fragments of the anti-Fc $\gamma$ RIIIA mAb 3G8 (24).

Here, we explored whether one could shift hFc $\gamma$ RIIA activation from ITAM signaling toward ITAMi signaling as a relevant therapeutic strategy in RA using transgenic mice expressing hFc $\gamma$ RIIA-R131. Anti-hFc $\gamma$ RIIA F(ab) $_2$  fragments or IVIg prevented RA development in these mice. The inhibitory mechanism was elucidated as induction of ITAMi signaling by hFc $\gamma$ RIIA independently of mFc $\gamma$ RIIB. Importantly, hFc $\gamma$ RIIA ITAMi signaling reversed the inflammatory phenotype of human synovial fluid-infiltrating cells from RA patients. Thus, switching hFc $\gamma$ RIIA from ITAM to ITAMi signaling opens new therapeutic perspectives in RA.

## Results

*Prevention of arthritis development in transgenic mice expressing hFc $\gamma$ RIIA following anti-hFc $\gamma$ RIIF(ab) $_2$  or IVIg treatment.* We first analyzed the effect of F(ab) $_2$  fragments of anti-hFc $\gamma$ RII mAb AT-10 on the development of CAIA in WT mice transgenic for hFc $\gamma$ RIIA-R131. MAb AT-10 is specific for hFc $\gamma$ RII, as compared with the monoclonal antibody IV.3, which specifically recognizes hFc $\gamma$ RIIA and not hFc $\gamma$ RIIB (Supplemental Figure 1; supplemental material available online with this article; doi:10.1172/JCI74572DS1). AT-10 F(ab) $_2$  treatment strongly inhibited arthritis development in transgenic mice expressing hFc $\gamma$ RIIA (hereafter referred to as hFc $\gamma$ RIIA<sup>Tg</sup>), but not in WT mice (Figure 1, A–E). Treatment with an irrelevant F(ab) $_2$  (clone 320) had no effect. Noticeably, AT-10 F(ab) $_2$  treatment reduced CAIA-induced ankle thickening to one-third of the level reached in WT mice (Figure 1C), implying that hFc $\gamma$ RIIA targeting might not only block potential deleterious activation of hFc $\gamma$ RIIA but might also counteract the activation triggered by the endog-

enous Fc $\gamma$ Rs. Morphological signs of cartilage destruction, synovitis, and pannus formation were significantly reduced in hFc $\gamma$ RIIA<sup>Tg</sup> mice by AT-10 F(ab) $_2$  treatment (Figure 1D).

To exclude the role of the endogenous activating (ITAM-bearing) Fc $\gamma$ Rs, the same experiments were performed in transgenic mice that express hFc $\gamma$ RIIA on the FcR $\gamma$ <sup>-/-</sup> background (having a genotype of Fc $\gamma$ 1<sup>-/-</sup>Fc $\gamma$ 2b<sup>-/-</sup>Fc $\gamma$ 3a<sup>-/-</sup>Fc $\gamma$ 1<sup>-/-</sup>Fc $\gamma$ 2<sup>-/-</sup>, hereafter referred to as hFc $\gamma$ RIIA<sup>Tg</sup>-FcR $\gamma$ <sup>-/-</sup> mice). Upon CAIA induction, hFc $\gamma$ RIIA<sup>Tg</sup>-FcR $\gamma$ <sup>-/-</sup> mice, but not FcR $\gamma$ <sup>-/-</sup> mice, fully developed arthritis (Figure 1, F and G), confirming the role of hFc $\gamma$ RIIA as a proinflammatory receptor in arthritis development as reported by others (25). In contrast, anti-hFc $\gamma$ RII AT-10 F(ab) $_2$  or a specific anti-hFc $\gamma$ RIIA IV.3 F(ab) $_2$ , but not irrelevant F(ab) $_2$ , treatment significantly inhibited arthritis development, as shown morphologically (Figure 1F and Supplemental Figure 2A) and by reduced ankle thickening (Figure 1G and Supplemental Figure 2B). Human IVIg similarly reduced arthritis development. More importantly, AT-10 F(ab) $_2$ -treated mice recovered rapidly from their low-score disease, whereas, within the time frame of the experiment, the disease reached a high-score plateau in control mice treated with irrelevant F(ab) $_2$ . This was accompanied by a significant reduction in leukocyte infiltration in the joints of hFc $\gamma$ RIIA<sup>Tg</sup> mice, particularly neutrophils and monocytes, as compared with WT mice (Figure 2, A–D).

To examine whether hFc $\gamma$ RIIA targeting inhibited chemotaxis of inflammatory leukocytes, we analyzed in vitro the transmigration of BM-derived macrophages (BMM). AT-10 F(ab) $_2$  treatment of BMM from hFc $\gamma$ RIIA<sup>Tg</sup>-FcR $\gamma$ <sup>-/-</sup> mice inhibited transmigration induced by MCP-1 (Figure 2E). As MCP-1 can also be produced by monocytes/macrophages, we examined the effect of AT-10 F(ab) $_2$  treatment on MCP-1 production by LPS-activated BMM. This production was also inhibited (Figure 2F). These findings suggest that AT-10 F(ab) $_2$  treatment might prevent both monocyte recruitment and activation of recruited monocytes, thereby blocking an inflammation-aggravating loop. This may explain, at least in part, the prevention of the development of arthritis in AT-10 F(ab) $_2$ -treated hFc $\gamma$ RIIA<sup>Tg</sup> mice.

*hFc $\gamma$ RIIA mediates ITAMi signaling that relies on the ITAM distal tyrosine.* To identify the mechanism through which hFc $\gamma$ RIIA targeting prevented arthritis development, we used BMM from hFc $\gamma$ RIIA<sup>Tg</sup>-FcR $\gamma$ <sup>-/-</sup> and FcR $\gamma$ <sup>-/-</sup> mice. Treatment of hFc $\gamma$ RIIA<sup>Tg</sup>-FcR $\gamma$ <sup>-/-</sup> BMM with AT-10 F(ab) $_2$  or with IVIg induced a transient recruitment (up to 30 minutes) of the protein tyrosine kinase Syk to hFc $\gamma$ RIIA, which was followed by stable recruitment (up to at least 6 hours) of the protein tyrosine phosphatase SHP-1 (Figure 3, A and B). These recruitments were accompanied by the concomitant phosphorylation of SHP-1. Neither AT-10 F(ab) $_2$  nor IVIg induced Syk or SHP-1 recruitment in the absence of Fc $\gamma$ RIIA (Figure 3, C and D). To analyze whether this signaling plays a role in the regulation of inflammation, we tested the effect of AT-10 F(ab) $_2$  and IVIg on the production of cytokines induced by LPS. Treatment of BMM with AT-10 F(ab) $_2$  or with IVIg inhibited the production of TNF- $\alpha$ , IL-6, and MIP-2 in hFc $\gamma$ RIIA<sup>Tg</sup>-FcR $\gamma$ <sup>-/-</sup> BMM but not in FcR $\gamma$ <sup>-/-</sup> BMM (Figure 3E). We confirmed these results using F(ab) $_2$  fragments of anti-hFc $\gamma$ RIIA mAb IV.3 (Supplemental Figure 2, C and D). This was associated with the inhibition of ROS production induced by N-formyl-methionine-leucine-phenylalanine (fMLF) from hFc $\gamma$ RIIA<sup>Tg</sup>-FcR $\gamma$ <sup>-/-</sup> BMM but not from FcR $\gamma$ <sup>-/-</sup>

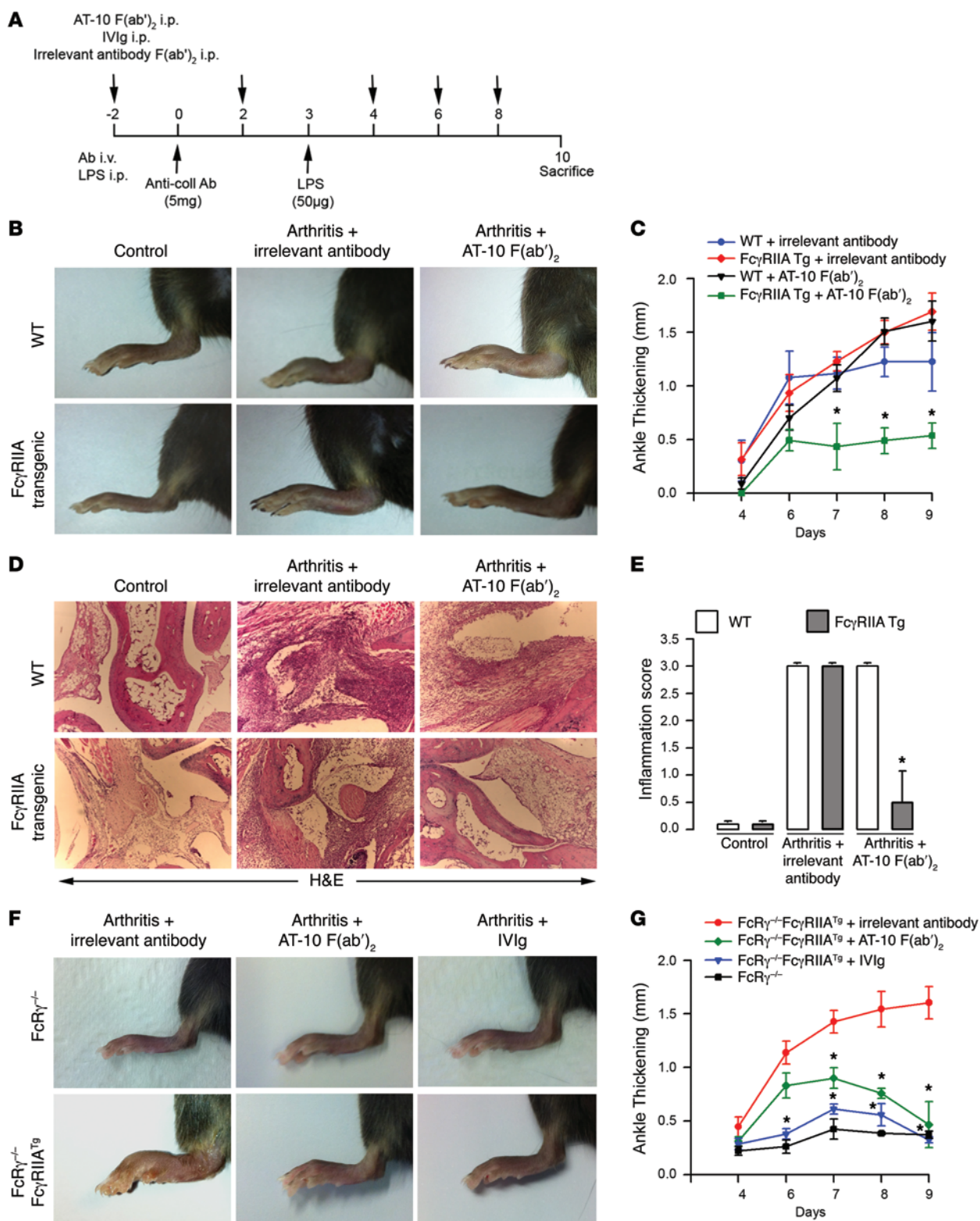


**Figure 1. Blocking F(ab')<sub>2</sub> fragments anti-hFcγRII or IVIg reduces edema and erythema as well as histological aspects of synovial hyperplasia in transgenic hFcγRIIA mice subjected to the CIA model.** (A) Arthritis protocol is shown. Mice were treated every 2 days with AT-10 F(ab')<sub>2</sub> or with an irrelevant mAb 320 F(ab')<sub>2</sub> (100 µg/20 g mouse) or IVIg (20 mg/20 g mouse) after disease induction by i.v. injection of an anti-CII mAb plus LPS. (B) Representative images of hind paws from WT (top panels) and hFcγRIIA<sup>Tg</sup> (bottom panels) mice at day 10. (C) Arthritis was evaluated by measuring the increase in ankle thickness (mm). Bars show mean ± SEM. (D) Microscopy analysis of H&E-stained tissue sections from ankles obtained from representative mice. Scale bars: 200 µm. (E) The inflammation scores were graded blind as follows: 0 (normal), 1 (mild), 2 (moderate), or 3 (severe). (F) Representative images of hind paws from FcγR<sup>-/-</sup> (top panels) and FcγRIIA<sup>Tg</sup>FcγR<sup>-/-</sup> mice (bottom panels) at day 10 after the initial injection of anti-CII mAb. (G) Arthritis was evaluated by measuring the increase in ankle thickness (mm). \*P < 0.05; n = 5.

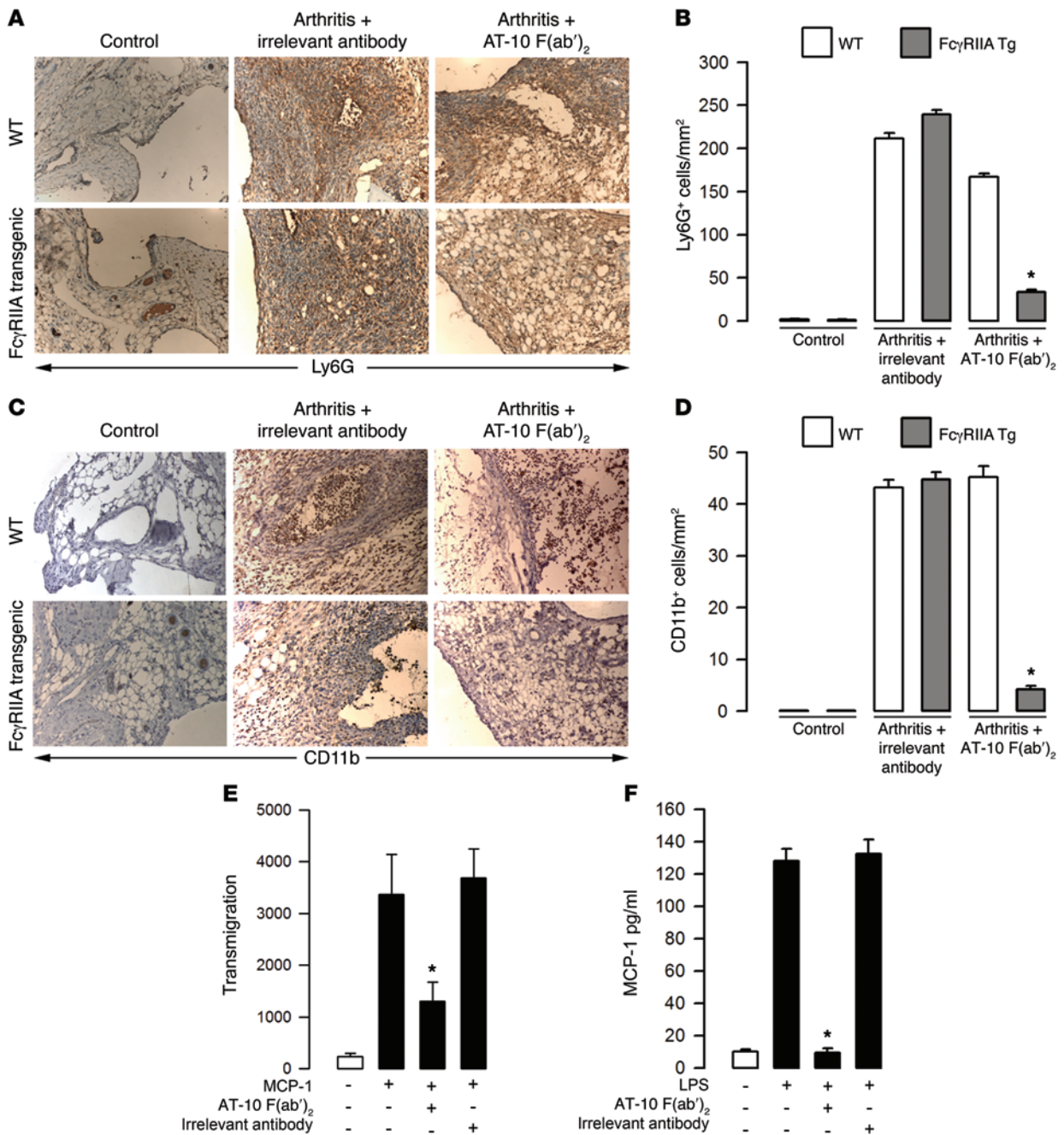


**Figure 2. In vivo hFcγRIIA targeting inhibits inflammatory cell infiltration in FcγRIIA<sup>Tg</sup> mice using a CAIA model.** (A) Gr-1 immunohistochemical staining (as indicated at the bottom) of hind paw sections from the indicated groups of mice. (B) Quantification of Gr-1-positive neutrophils. (C) CD11b immunohistochemical staining of hind paw sections from the indicated groups of mice. Scale bars: 10 μm. (D) Quantification of CD11b-positive monocytes/macrophages. (E) Chemotaxis response: BMM from FcγRIIA<sup>Tg</sup>-FcRγ<sup>-/-</sup> mice were pretreated in the upper chamber with AT-10 F(ab)<sub>2</sub> or irrelevant F(ab)<sub>2</sub> for 30 minutes (10 μg/ml). MCP-1 was added to the lower chamber, and the number of transmigrated cells was quantified. (F) MCP-1 production: BMM from FcγRIIA<sup>Tg</sup>-FcRγ<sup>-/-</sup> mice were stimulated by LPS in the presence of AT-10 F(ab)<sub>2</sub> or irrelevant F(ab)<sub>2</sub> for 30 minutes, and the released MCP-1 was measured by ELISA. \*P < 0.05; n = 5.

BMM (Supplemental Figure 2E). Thus, targeting of hFcγRIIA on mouse BMM induced ITAm1 signaling responsible for inhibition of an inflammatory response such as the one observed during arthritis development in mice.

To determine whether targeting of hFcγRIIA could induce inhibitory signaling in human monocytes, we used the THP-1 monocytic cell line transfected with hFcγRIIA-R131 (THP-1-FcγRIIA-R131<sup>+</sup>-

CD14<sup>+</sup>) (26). These cells express hFcγRI and hFcγRIIA but neither hFcγRIIB nor hFcγRIII (Figure 4A). Whereas targeting of hFcγRIIA with Fab fragments of AT-10 did not induce any signaling (data not shown), preincubation of the cells with AT-10 F(ab)<sub>2</sub> induced a transient recruitment of the tyrosine kinase Syk to hFcγRIIA, followed by stable recruitment and tyrosine phosphorylation of the tyrosine phosphatase SHP-1 (Figure 4B). No recruitment of the SH2-con-

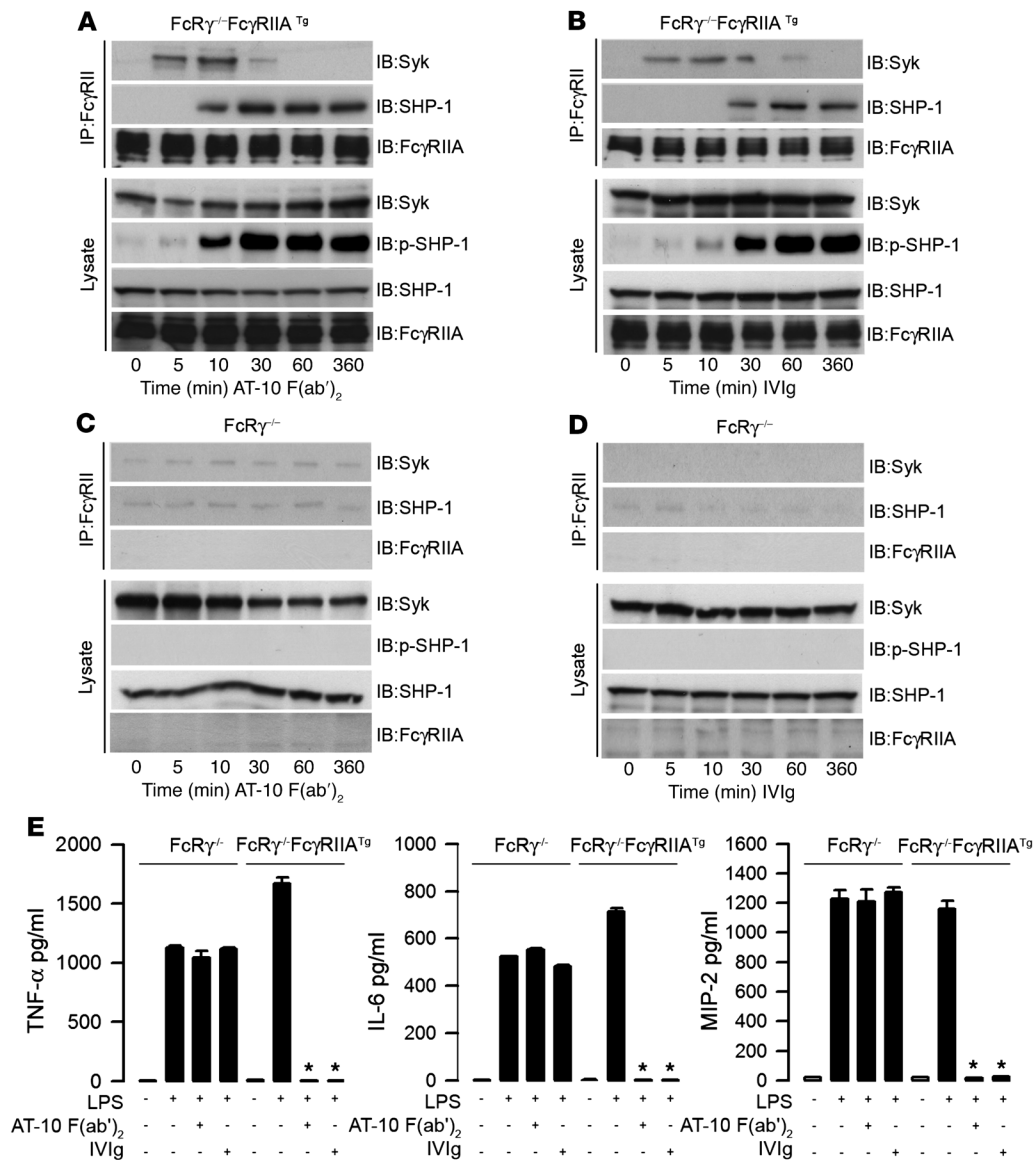


**Figure 3. hFcγRIIA targeting by anti-hFcγRII F(ab)<sub>2</sub> or IVIg induces SHP-1-dependent inhibitory signaling that blocks LPS-induced proinflammatory cytokine production by mouse macrophages.** BMM from hFcγRIIA<sup>Tg</sup>-FcγRII<sup>-/-</sup> (A and B) or FcγRII<sup>-/-</sup> (C and D) mice were incubated with either AT-10 anti-hFcγRII F(ab)<sub>2</sub> (10 μg/ml; A and C) or IVIg (10 mg/ml; B and D) for the indicated times at 37°C. Cells were solubilized in 1% digitonin lysis buffer and immunoprecipitated with AT-10 (IP: FcγRII). Eluted proteins were immunoblotted (IB) with antibodies of the indicated specificities. Total lysates were analyzed likewise by immunoblotting. (E) Cytokine production: 2 × 10<sup>6</sup> BMM from hFcγRIIA<sup>Tg</sup>-FcγRII<sup>-/-</sup> or FcγRII<sup>-/-</sup> mice were pretreated, or not, with AT-10 F(ab)<sub>2</sub> (10 μg/ml) or IVIg (10 mg/ml) for 30 minutes and stimulated for 6 hours with 10 ng/ml of LPS. Release of TNF-α, IL-6, and MIP-2 was measured by ELISA. \*P < 0.05.

taining 5-inositol phosphate phosphatase SHIP1 to hFcγRIIA was observed. Confirming the role of hFcγRIIA in Syk and SHP-1 recruitment in these cells, silencing *FCGR2A* mRNA (encoding hFcγRIIA) abolished Syk and SHP-1 recruitment (Figure 4C). A control siRNA had no effect (Supplemental Figure 3). Silencing Syk expression (Figure 4D) impaired the recruitment of SHP-1 to hFcγRIIA induced by AT-10 F(ab)<sub>2</sub> (Figure 4E). Together, these findings suggest that in hFcγRIIA, targeting by AT-10 F(ab)<sub>2</sub> induced an inhibitory signaling pathway (independently of FcγRIIB) sequentially involving Syk and SHP-1, as previously described for ITAMi signaling of FcγR-associated Fc receptors (24).

Because hFcγRIIA is a single-transmembrane (single-TM) receptor possessing 3 tyrosine residues in its cytoplasmic tail,

2 of which are conserved tyrosine residues arranged in a non-canonical ITAM, we explored whether the hFcγRIIA inhibitory signal was dependent on the hFcγRIIA-ITAM tyrosine residues. We transfected the rat basophilic leukemia cell line RBL-2H3 with WT hFcγRIIA or with hFcRIIA mutated on each of the 3 intracellular tyrosine residues. All transfectants expressed significant levels of the respective hFcγRIIA mutants at the cell surface (Figure 5A and Supplemental Figure 4A). As expected, targeting of transfectants expressing WT hFcγRIIA with AT-10 F(ab)<sub>2</sub> resulted in sequential recruitment of Syk and SHP-1 to the receptor (Figure 5B). AT-10 F(ab)<sub>2</sub> treatment also induced inhibition of cell activation triggered by a nontargeted activating receptor. Indeed, degranulation (β-hexosaminidase release) induced upon crosslinking of the

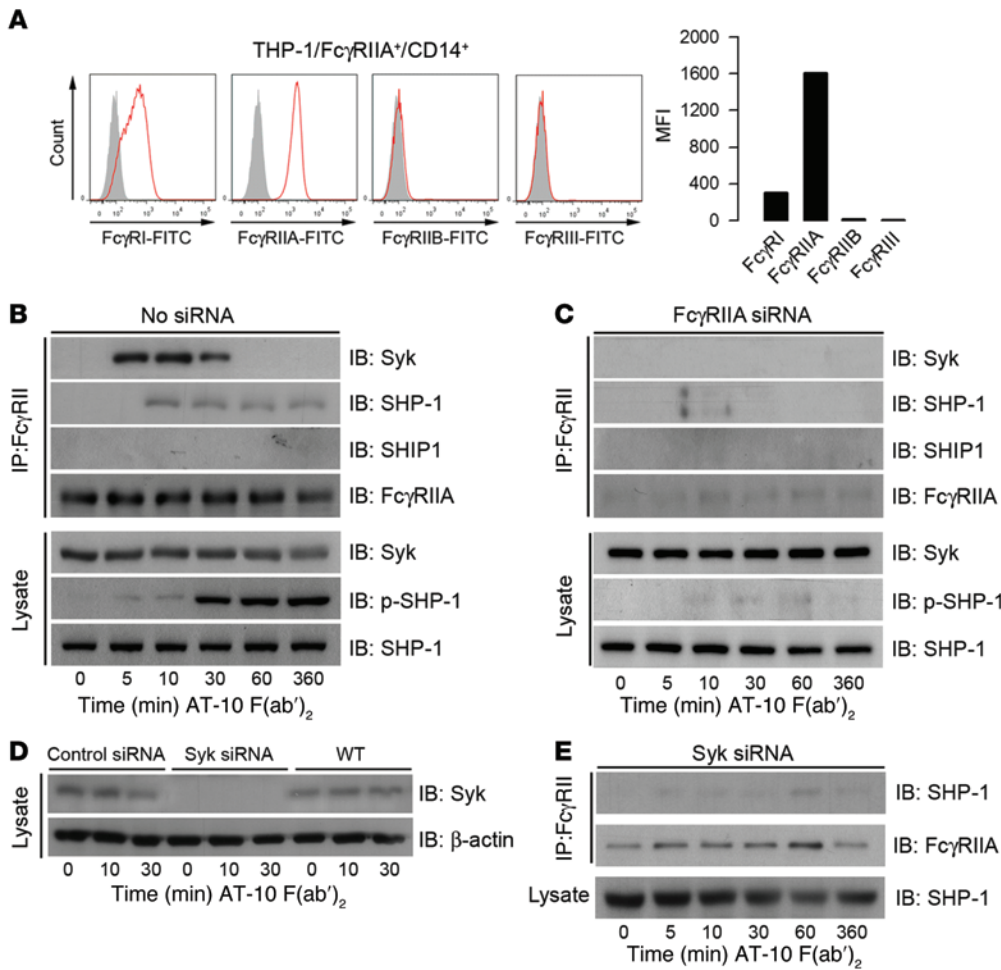


**Figure 4. hFcγRIIA targeting by anti-hFcγRII F(ab')<sub>2</sub> induces inhibitory signaling in a human monocyte cell line.** (A) Representative expression of FcγRs on THP-1-hFcγRIIA-R131<sup>+</sup>-CD14<sup>+</sup> cells. Gray-shaded histograms represent staining with isotype controls; open red histograms represent hFcγRI, hFcγRIIA, hFcγRIIB, and hFcγRIII staining, respectively. Quantification is shown in the right panel. (B–E) THP-1-hFcγRIIA-R131<sup>+</sup>-CD14<sup>+</sup> cells transfected with the indicated siRNA were incubated for the indicated times with AT-10 F(ab')<sub>2</sub> (10 μg/ml) at 37°C. Cells were solubilized in 1% digitonin lysis buffer. Lysates were immunoprecipitated with AT-10 antibody (IP: FcγRII). Eluted proteins and total lysates were analyzed by immunoblotting with antibodies of the indicated specificities.

high-affinity IgE receptor (FcεRI) by IgE and antigen was strongly inhibited (65% inhibition) following AT-10 F(ab')<sub>2</sub> treatment (Figure 5C). The Y304F (Y-to-F mutation at position 304 located in hFcγRIIA ITAM) was sufficient to abolish both the inhibitory signal induced by AT-10 F(ab')<sub>2</sub> (Figure 5B) and to restore degranulation (Figure 5C). The Y288F (first tyrosine of the ITAM) or Y281F (TM region-proximal tyrosine) did not induce such effects. In contrast, both ITAM tyrosine residues (Y288 and Y304) were required for cell activation following extensive aggregation of hFcγRIIA (independently of FcεRI triggering) as measured by stable Syk recruitment, absence of SHP-1 recruitment, and cell degranulation (Figure 5, D and E). Double and triple mutants of these tyrosine residues confirmed these results (Supplemental Figure 4, B–G).

Together, these findings demonstrate that hFcγRIIA can initiate an inhibitory signaling that has all the characteristics of bona fide ITAMi signaling, including sequential Syk–SHP-1 recruitment, inhibition of heterologous receptors (such as FcεRI or TLR4), and requirement for an intact ITAM motif. Furthermore, these data unveil different structural requirements for ITAM activating and ITAMi signals generated by hFcγRIIA.

*Both hFcγRIIA R131 and H131 allotypes mediate ITAMi signaling.* FcγRIIA exhibits a genetically determined polymorphism (FcγRIIA-R131 and FcγRIIA-H131), resulting in differential ability to bind IgG subclasses (12). To explore whether these 2 allotypes can induce ITAMi signaling, we established RBL-2H3 transfectants

expressing either hFcγRIIA-R131 or hFcγRIIA-H131. In both transfectants, which expressed significant levels of these allotypes at their cell surface (Figure 4A and Figure 6A), targeting the receptor by AT-10 F(ab')<sub>2</sub> resulted in a similar ITAMi signature with Syk transient recruitment and SHP-1 stable recruitment (Figure 6B). Moreover, IgE-mediated degranulation of hFcγRIIA-R131<sup>+</sup> or hFcγRIIA-H131<sup>+</sup> RBL-2H3 transfectants was similarly inhibited by AT-10 F(ab')<sub>2</sub> treatment (93% and 82% inhibition, respectively) (Figure 6C). Overall, these data demonstrate that both FcγRIIA allotypes can induce ITAMi signaling and similarly inhibit cell activation.

*hFcγRIIA-ITAMi signaling prevents IRAK-1-induced inflammatory responses.* Leukocyte infiltration in the inflamed synovium, one of the hallmarks of severe RA, is linked to disease progression and characterized by exacerbated production of inflammatory cytokines and ROS (27). To explore whether hFcγRIIA-induced inhibitory signaling resulted in the modulation of leukocyte inflammatory response, we first analyzed the production of cytokines in LPS-stimulated THP-1-hFcγRIIA-R131<sup>+</sup>-CD14<sup>+</sup> cells and in purified blood monocytes transfected or not with various siRNA and stimulated with 10 ng/ml of LPS. Pretreatment of THP-1-hFcγRIIA-R131<sup>+</sup>-CD14<sup>+</sup> cells with AT-10 F(ab')<sub>2</sub> nearly abolished IL-8 secretion induced by LPS (Figure 7A). Silencing of the mRNA encoding hFcγRIIA, Syk, or SHP-1 significantly restored IL-8 production induced by LPS in these conditions (Figure 7A). Likewise,



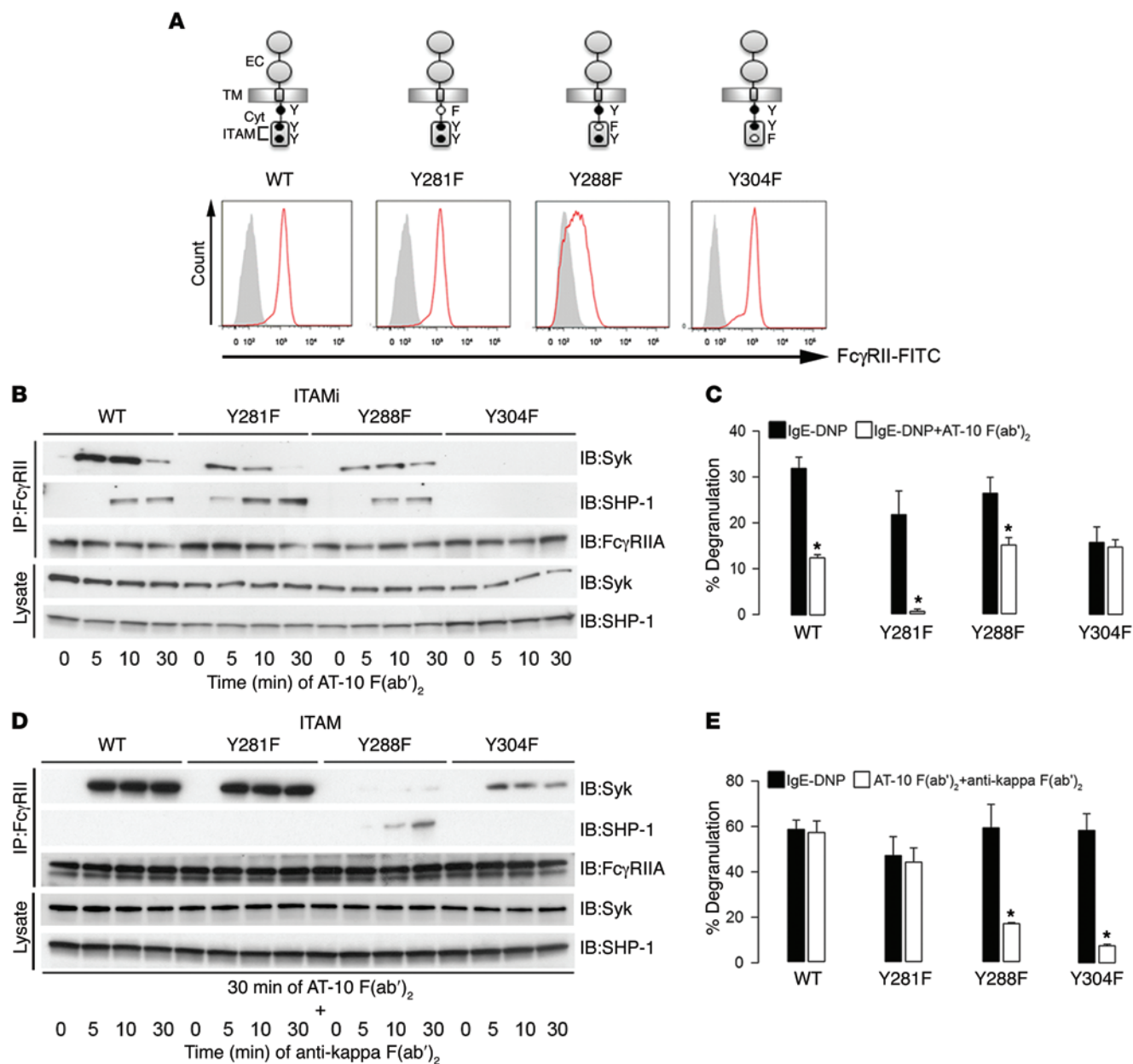


**Figure 5. hFc $\gamma$ RIIA mediates inhibition that relies on the ITAM distal tyrosine.** (A) hFc $\gamma$ RIIA constructs are schematically represented; their surface-expression levels after transfection into RBL-2H3 cells are shown compared with nontransfected cells (gray-shaded vs. open red histograms). (B) For ITAMi induction, RBL-2H3 transfectants were incubated at 37°C with AT-10 F(ab) $_2$  (10  $\mu$ g/ml) for indicated times; cell lysates were immunoprecipitated with AT-10 (IP: Fc $\gamma$ RII) followed by immunoblotting with anti-Syk, anti-SHP-1, or anti-hFc $\gamma$ RIIA. The amounts of SHP-1 and Syk in lysates were analyzed in parallel by immunoblotting. (C) IgE-sensitized RBL-2H3 transfectants were incubated overnight at 37°C with AT-10 F(ab) $_2$ , and degranulation was triggered with DNP-HSA for 45 minutes. Net  $\beta$ -hexosaminidase release was determined. (D) For ITAMa induction, RBL-2H3 transfectants were incubated with AT-10 F(ab) $_2$  for 30 minutes at 4°C, washed, and stimulated with anti-mouse  $\kappa$  chain F(ab) $_2$  for the indicated times at 37°C. Cells lysates were treated and analyzed as in B. (E) RBL-2H3 transfectants were incubated with AT-10 F(ab) $_2$  (10  $\mu$ g/ml) for 30 minutes at 4°C, and degranulation was triggered by anti- $\kappa$  F(ab) $_2$  for 45 minutes at 37°C. In parallel, IgE-sensitized RBL-2H3 transfectants were treated as in C. \* $P$  < 0.05;  $n$  = 12.

pretreatment of purified human blood monocytes with AT-10 F(ab) $_2$  significantly impaired the LPS-induced secretion of TNF- $\alpha$ , IL-6, and IL-8 independently of Fc $\gamma$ RIIB, as a FCGR2B knockdown had no effect on AT-10-mediated inhibition in monocytes (data not shown). Again, siRNA-induced knockdown of the mRNAs encoding hFc $\gamma$ RIIA, Syk, or SHP-1 restored the LPS-induced production of these inflammatory cytokines (Figure 7B). Efficacy of siRNAs for FCGR2A and FCGR2B was verified by reverse tran-

scriptase PCR (RT-PCR) in blood monocytes (Supplemental Figure 5). To further elucidate the hFc $\gamma$ RIIA inhibitory mechanism involved in the downregulation of responses to LPS, TLR4-signaling pathways were investigated. AT-10 F(ab) $_2$  inhibited the activation and degradation of IL-1 receptor-associated kinase 1 (IRAK-1) and the phosphorylation of NF- $\kappa$ B (p65) induced by LPS in THP-1-hFc $\gamma$ RIIA-R131 $^+$ -CD14 $^+$  cells (Figure 7C). This was associated with SHP-1 phosphorylation. Moreover, silencing of Syk or SHP-1 by

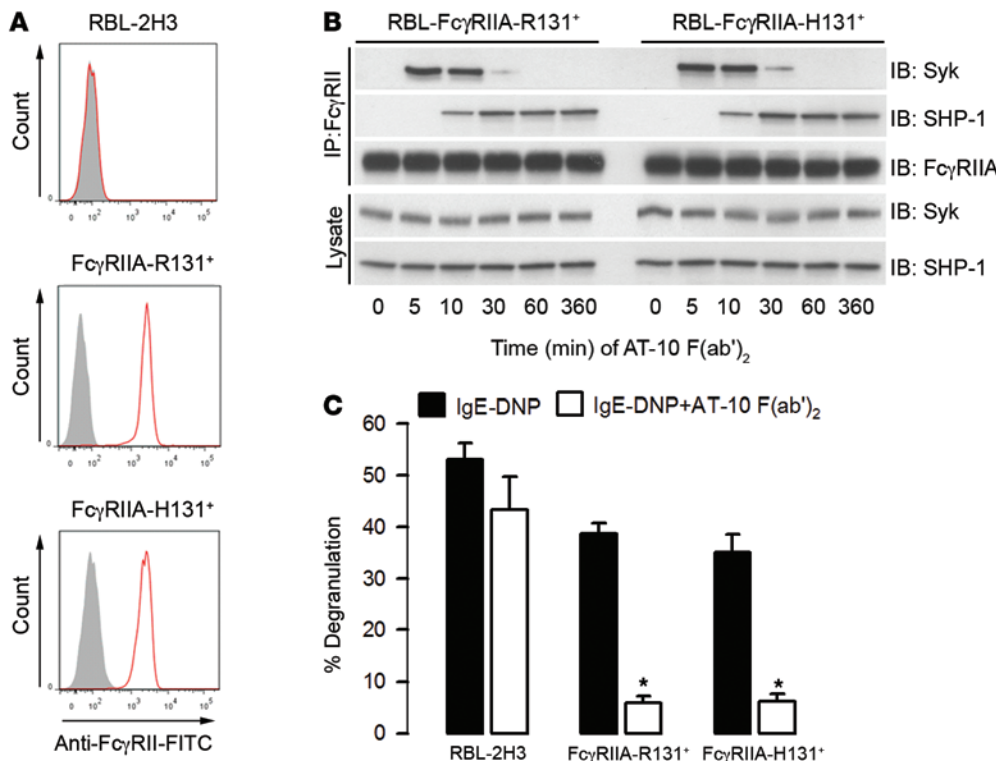


**Figure 6. Both hFcγRIIA R131 and H131 allotypes mediate ITAMi signaling.** (A) Surface-expression levels of hFcγRIIA allotypes in RBL-2H3 transfectants are shown compared with nontransfected cells (gray-shaded vs. open red histograms). (B) For ITAMi analysis, RBL-2H3 transfectants were incubated at 37°C with AT-10 F(ab)<sub>2</sub> (10 μg/ml) for the indicated times; FcγRIIA was immunoprecipitated from cell lysates with AT-10 (FcγRII) followed by immunoblotting with anti-Syk, anti-SHP-1, or anti-hFcγRIIA. The amount of SHP-1 and Syk in lysates was analyzed in parallel by immunoblotting. (C) IgE-sensitized RBL-2H3 transfectants were incubated overnight at 37°C with AT-10 F(ab)<sub>2</sub>, and degranulation was triggered with DNP-HSA for 45 minutes. Net β-hexosaminidase release was determined. \*P < 0.05.

siRNA restored the activation of IRAK-1 and the phosphorylation of p65, confirming that ITAMi signaling may control TLR-signaling effectors. Next, IRAK-1 was immunoprecipitated to explore the effect of ITAMi signaling on LPS-induced IRAK-1-TRAF-6 association and a possible interaction between IRAK-1 and SHP-1. Pretreatment of THP-1-hFcγRIIA-R131<sup>+</sup>-CD14<sup>+</sup> cells with AT-10 F(ab)<sub>2</sub> induced an interaction between SHP-1 and IRAK-1 and impaired the formation of the IRAK-1-TRAF-6 complex induced by LPS. Silencing of SHP-1 or of Syk by siRNA impaired the ITAMi-induced effects (Figure 7D).

These results demonstrate that hFcγRIIA-ITAMi signaling inhibits LPS-induced IRAK-1 activation, resulting in the blockade of NF-κB activation and in the dampening of inflammatory responses in monocytes (summarized in Figure 7E).

*hFcγRIIA-ITAMi signaling regulates ROS production through inhibition of Vav-1 and Rac.* Next, we examined whether hFcγRIIA-ITAMi signaling could modulate ROS production by primary human blood neutrophils that abundantly express hFcγRIIA and the glycosylphosphatidylinositol-linked (GPI-linked) hFcγRIIIB, but neither hFcγRIIIB nor hFcγRI (Figure 8A). As Vav-1 and the small GTPase Rac play key roles in the production of ROS (28, 29), we investigated the impact of hFcRIIA ITAMi signaling on these molecules. Pretreatment of neutrophils with AT-10 F(ab)<sub>2</sub> inhibited both constitutive and fMLF-induced ROS production (Figure 8B). This was associated with impaired interactions between Rac and Vav-1 and between Rac and PAK-1 (Figure 8C). As SHP-1 selectively dephosphorylates Vav-1 during inhibitory signaling induced by killer cell inhibitory receptors in NK cells (30), we next investigated whether hFcRIIA-ITAMi-recruited SHP-1 may target Vav-1. AT-10 F(ab)<sub>2</sub> treatment induced a Vav-1-SHP-1 interaction (Figure 8D). To explore whether hFcγRIIIB may contribute to this inhibitory path-

way, we used primary blood monocytes that, unlike human neutrophils, express this inhibitory receptor (Figure 8E). These cells use the same signaling pathway, leading to ROS production following fMLF stimulation. As expected, AT-10 F(ab)<sub>2</sub> inhibited ROS production in primary monocytes (Figure 8F). FCGR2B siRNA had no effect on this inhibition (Figure 8F and Supplemental Figure 5). In contrast, SHP-1 silencing by siRNA restored ROS production. As observed for neutrophils, pretreatment of monocytes with AT-10 F(ab)<sub>2</sub> inhibited the fMLF-induced interactions between Rac and Vav-1 and between Rac and PAK-1 (Figure 8G) that correlated with the induction of a Vav-1-SHP-1 interaction (Figure 8H). Additionally, SHP-1 silencing by siRNA restored Rac-Vav-1 interaction and consequently Rac-PAK1 complex formation (Figure 8G). These data show that hFcγRIIA targeting by AT-10 F(ab)<sub>2</sub>, independently of inhibitory hFcγRIIB, induces an ITAMi signaling that is responsible for the recruitment of SHP-1, leading, through inhibition of Vav-1, to blocking of Rac activation, resulting in a decrease of ROS production in human blood monocytes and neutrophils (Figure 8I).

*Reverting synovial cell activation from RA patients by hFcγRIIA-ITAMi induction.* RA is associated with an infiltration of blood cells and ROS production in the synovial compartment, all of which are responsible for tissue injury and disease severity (2). Neutrophils accounted for the majority (75%) of infiltrating cells in the synovium of RA patients, whereas monocytes were a minority (6%), with T cells accounting for the remaining cells. Infiltrating neutrophils expressed high levels of hFcγRIIA and GPI-linked hFcγRIIIB and very low levels of hFcγRI and hFcγRIIIB, whereas infiltrating monocytes expressed high levels of hFcγRI and hFcγRIIA and significant levels of hFcγRIIIB and hFcγRIII (Figure 9A). As expected, infiltrating T cells expressed no hFcγR. ROS are constitutively produced by infiltrating cells isolated from the synovial fluid of RA patients.

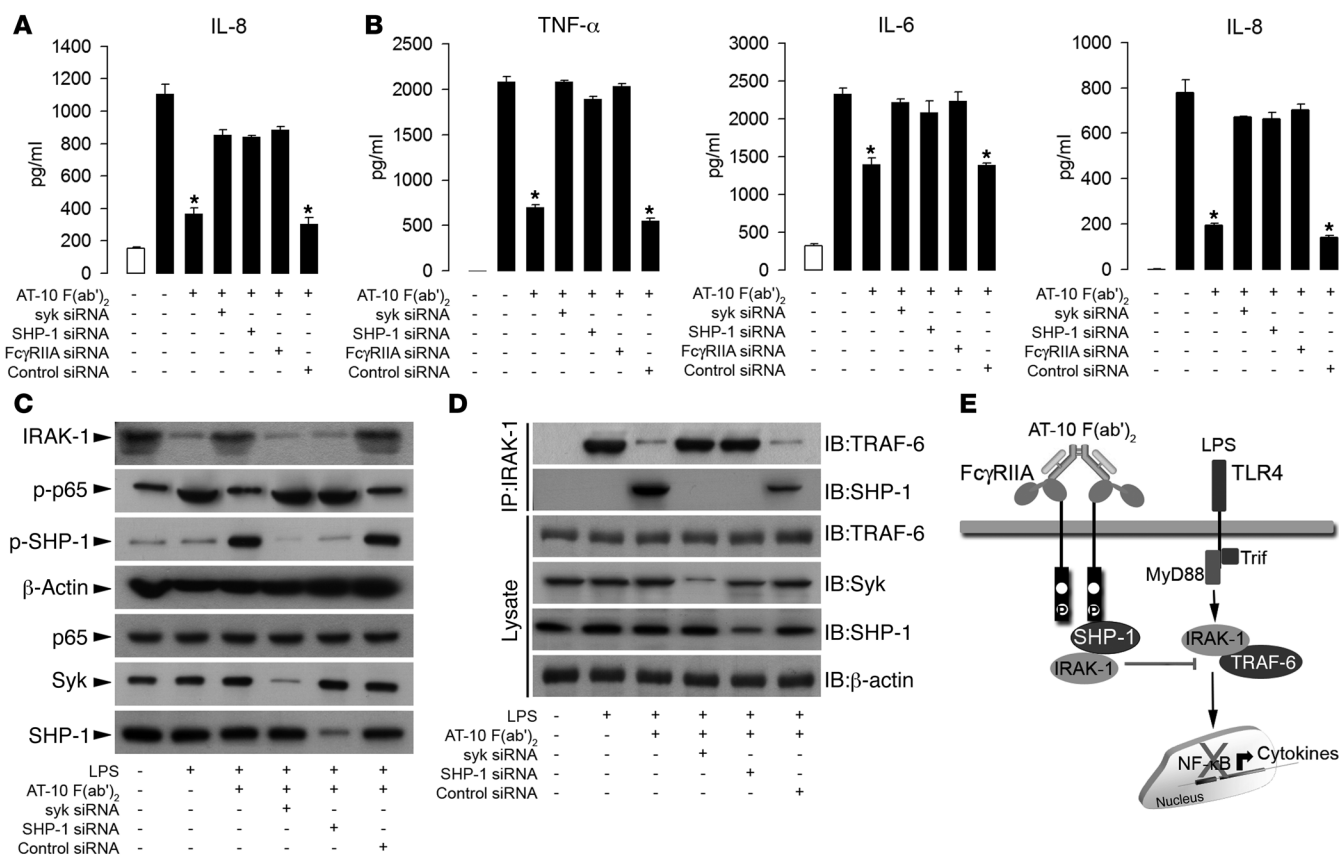


**Figure 7. hFcγRIIA-ITAMi signaling modulates inflammatory responses through inhibition of IRAK-1.** (A) THP-1-hFcγRIIA-R131<sup>+</sup>-CD14<sup>+</sup> cells transfected or not with the indicated siRNA were incubated with AT-10 F(ab')<sub>2</sub> for 30 minutes before addition of LPS (10 ng/ml) for 6 hours. Released IL-8 was measured by ELISA. (B) Blood monocytes were transfected with the indicated siRNA, incubated with AT-10 F(ab')<sub>2</sub> for 30 minutes, and stimulated with LPS (10 ng/ml) for 6 hours. TNF-α, IL-6, and IL-8 levels in cell supernatants were measured by ELISA. (C) THP-1-hFcγRIIA-R131<sup>+</sup>-CD14<sup>+</sup> cells were transfected with the indicated siRNA and pretreated with AT-10 F(ab')<sub>2</sub> (10 μg/ml) for 30 minutes, followed by LPS for 15 minutes. Immunoblot analysis of the indicated proteins in cell lysates is represented. (D) THP-1-hFcγRIIA-R131<sup>+</sup>-CD14<sup>+</sup> cells were treated and stimulated as described in C, and cell lysates were subjected to immunoprecipitation using anti-IRAK-1 antibody (IRAK-1). Eluates and cell lysates were immunoblotted with antibodies specific for the indicated proteins. (E) Proposed mechanism by which hFcγRIIA-mediated ITAMi signalling regulates the LPS-induced proinflammatory response. \*P < 0.05. Data in blots are from 1 representative out of 3 independent experiments.

Strikingly, AT-10 F(ab')<sub>2</sub> inhibited this constitutive ROS production (Figure 9B). AT-10 F(ab')<sub>2</sub> also inhibited the constitutive interaction of Rac with Vav-1 and PAK-1 in these cells (Figure 9C). Immunoprecipitation of hFcγRIIA from the lysates of patient infiltrating cells revealed that Syk was constitutively associated with hFcRIIA (Figure 9D). A constitutive activation state of this receptor, leading to Syk association, can be explained by constant triggering by IgG ICs present in RA synovial fluids. The association of SHP-1 with hFcγRIIA was, however, detected only after AT-10 F(ab')<sub>2</sub> treatment. In contrast, in blood cells from a healthy donor, SHP-1 was constitutively associated with hFcγRIIA, whereas no association of Syk with hFcγRIIA was observed (Figure 9D). To determine whether the targeting of hFcγRIIA can reverse the classical ITAM-signaling pathway observed in infiltrating cells isolated from the synovial fluid of RA patient 2, we treated these cells with AT-10 F(ab')<sub>2</sub> for 30 minutes to 2 hours. AT-10 F(ab')<sub>2</sub> induced a transient increase in Syk recruitment, but a stable (at least 2 hours) recruitment of SHP-1 (Figure 9E). As a control, a similar treatment induced the same ITAMi signals in blood cells from healthy donor 2 (Figure 9F). AT-10 F(ab')<sub>2</sub> also prevented fMLF-induced stimulation of these

infiltrating cells, as revealed by reduced ROS production and increased association among Rac, Vav-1, and PAK-1 (Figure 9, B and C). These observations show that AT-10 F(ab')<sub>2</sub> treatment switches the constitutive inflammatory FcγRIIA-ITAM “activation” signaling into a “FcγRIIA-ITAMi” signaling in infiltrating cells from RA patients, thus reverting Rac activation and ROS production and opening new therapeutic avenues in this disease.

**Discussion**

Our data demonstrate that hFcγRIIA (CD32A) can function as both an activating and an inhibitory receptor. By modifying the type of receptor engagement, one may switch the function of this dual activating/inhibitory receptor and use that property to revert the inflammatory phenotype of hFcγRIIA-expressing cells, as we demonstrated for infiltrating cells from the synovial cavity of RA patients. Synovial fluid-infiltrating cells from RA patients displayed constitutive ITAM activation (that we propose to name “ITAMa”) of hFcγRIIA, as revealed by constitutive activation of the signaling pathway leading to ROS production. In contrast, blood leukocytes from healthy donors showed a constitutive

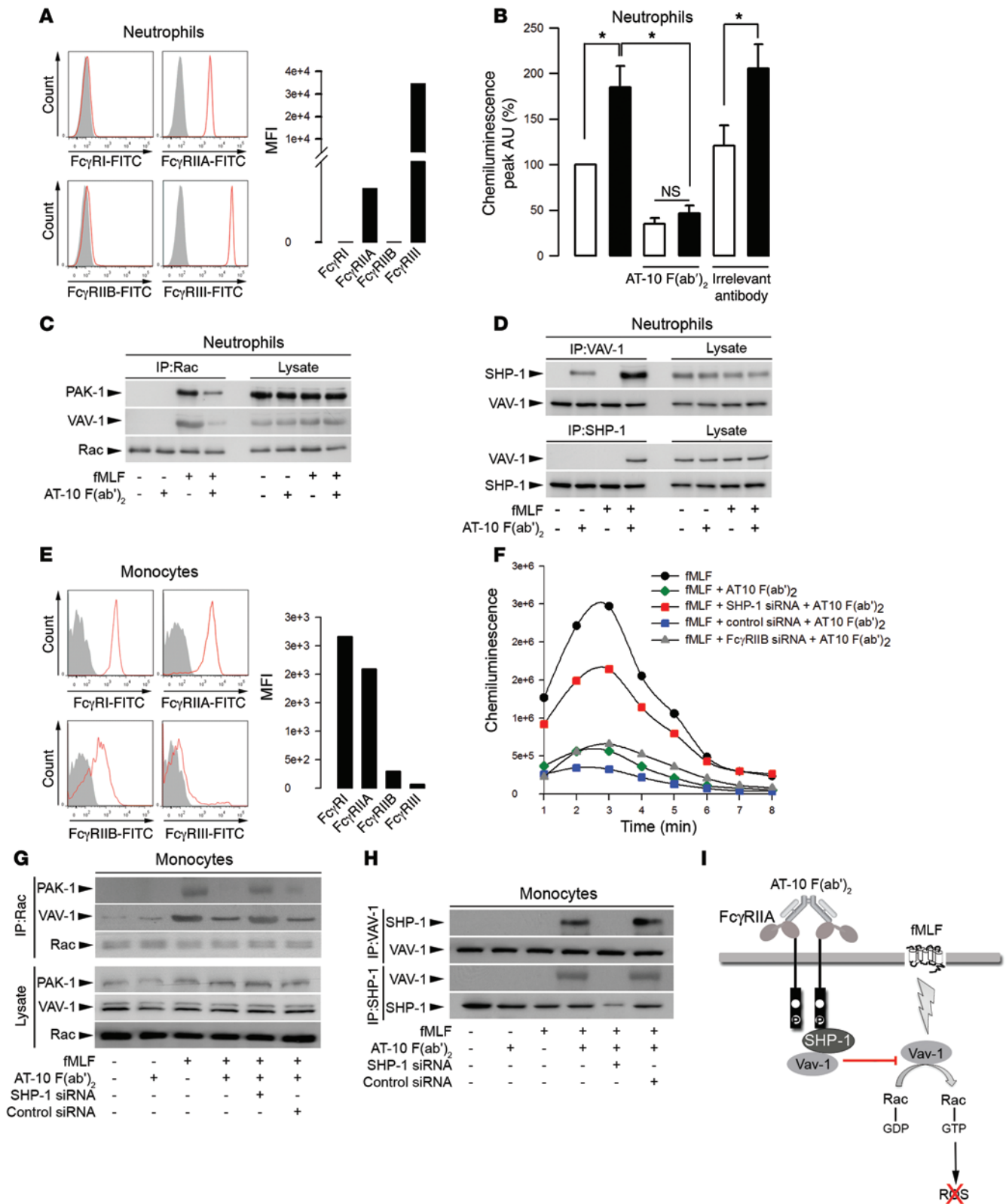


**Figure 8. hFc $\gamma$ RIIA-ITAMi signaling regulates ROS production through inhibition of Vav-1 and Rac.** (A) Representative hFc $\gamma$ R expression on human neutrophils. Gray-shaded histograms represent staining with isotype controls; open red histograms show hFc $\gamma$ RI, hFc $\gamma$ RIIA, hFc $\gamma$ RIIB, and hFc $\gamma$ RIII staining, respectively. Right panel indicates quantification by mean fluorescence intensity (MFI). (B) ROS production by human neutrophils preincubated with indicated antibody before cell activation with fMLF. Peak of ROS production was measured by luminol-amplified chemiluminescence. (C) Neutrophil cell lysates were subjected to anti-Rac immunoprecipitation, and eluted proteins were analyzed by immunoblotting with indicated antibodies. Cell lysates were also analyzed by immunoblotting. (D) Neutrophil cell lysates treated as in C were subjected to anti-Vav-1 or anti-SHP-1 immunoprecipitation. Eluted proteins were analyzed by immunoblotting for the presence of indicated proteins. (E) Cell lysates were also analyzed by immunoblotting. (F) Representative hFc $\gamma$ R expression on human monocytes as in A. (G) ROS production by human monocytes transfected with the indicated siRNA as in B. (H and I) Lysates from human monocytes transfected with the indicated siRNA were preincubated with AT-10 F(ab)<sub>2</sub> before cell activation with fMLF. (G) Monocyte cell lysates were subjected to anti-Rac immunoprecipitation. Eluted material was analyzed by immunoblotting for the presence of indicated proteins. Cell lysates were also analyzed by immunoblotting. (H) Monocyte cell lysates were subjected to immunoprecipitation with indicated antibodies and analyzed by immunoblotting for the presence of indicated proteins. (I) Proposed mechanism by which hFc $\gamma$ RIIA-mediated ITAMi signaling regulates ROS production induced by fMLF. \**P* < 0.05. Data represent 1 of 3 independent experiments.

“ITAMi” configuration of hFc $\gamma$ RIIA that requires involvement of the tyrosine phosphatase SHP-1. ITAM-dependent recruitment of SHP-1 has been previously demonstrated following activation of Fc $\epsilon$ RI or hFc $\gamma$ RIIA (31, 32) and is thought in this case to act as a negative feedback loop regulating activation signals induced by their own receptors in an intrinsic retro-control mechanism. This differs substantially from the hFc $\gamma$ RIIA-ITAMi configuration in which SHP-1 acts toward a heterologous receptor. This configuration can be induced with AT-10 F(ab)<sub>2</sub> even when receptors are already activated in vivo by ICs. This switch from an “ITAMa” to an “ITAMi” configuration in RA synovial fluid-infiltrating cells led to an inhibition of ROS production (Figure 10). This mechanism may explain the significant therapeutic effect following AT-10 F(ab)<sub>2</sub> treatment that we observed in the mouse model of RA. Interestingly, hFc $\gamma$ RIIA blockade by small chemical inhibitors as antagonists attenuates arthritis (33). However, the inhibitory signal investigated in this study seems to rely on its passive blocking effect rather than on ITAMi signaling since, in contrast with ITAMi signaling (18), it failed to inhibit activation of heterologous receptors.

Human Fc $\gamma$ RIIA exhibit a genetically determined polymorphism (hFc $\gamma$ RIIA-R131 and hFc $\gamma$ RIIA-H131) (12, 34), resulting in differential ability to recognize and be activated by human and murine IgG isotypes. The H131 allele has a moderate affinity for human IgG2 and a low affinity for murine IgG1, while the R131 allele has a low affinity for human IgG2, but a moderate affinity for murine IgG1 (9, 12). The current study is the first, to our knowledge, to demonstrate that targeting of either allele by AT-10 F(ab)<sub>2</sub> is able to induce ITAMi signaling, indicating that hFc $\gamma$ RIIA polymorphism does not influence the antiinflammatory effect of anti-Fc $\gamma$ RIIA antibodies. This approach could thus be used as a treatment for RA patients independently of *FCGR2A* polymorphisms.

Circulating autoantibodies are a prominent feature of RA, and joint tissue is frequently covered with ICs (3, 4). It has been clearly demonstrated that ITAM-bearing Fc receptors are crucial for arthritis development in mice. Indeed, mice lacking the Fc $\gamma$  subunit that is required for the expression of activating mouse FcRs (Fc $\gamma$ <sup>-/-</sup> mice) were resistant to K/BxN (35) and CAIA (15, 36) arthritis. In humans, hFc $\gamma$ RIIA, and more particularly, hFc $\gamma$ RIIA-R131, is associated with RA development (15). However, as mice do not express hFc $\gamma$ RIIA, the transgenic expression of hFc $\gamma$ RIIA was established to develop a mouse model relevant to the human RA disease (37). We confirm here that transgenic mice expressing hFc $\gamma$ RIIA alone on a Fc $\gamma$ <sup>-/-</sup> background were prone to developing arthritis. Importantly, we show for what we believe is the first time that an inhibitory signal generated by the same receptor was effective in vivo, as treatment of CAIA in these mice by AT-10 or IV.3 F(ab)<sub>2</sub> resulted in a significant reduction of inflammation and arthritic scores. These antibodies do not bind murine Fc $\gamma$ RIIB, excluding its contribution in these experiments. Interestingly, ICs formed by the interaction of disease-specific autoantibodies to citrullinated proteins with, for example, citrullinated fibrin, activate hFc $\gamma$ RIIA ITAM, contributing to TNF- $\alpha$  production by macrophages (25). This activation process could be blocked by anti-hFc $\gamma$ RIIA F(ab)<sub>2</sub>, but neither by anti-hFc $\gamma$ RI nor anti-hFc $\gamma$ RIII antibodies. Our data demonstrate that such a treatment not only alleviated hFc $\gamma$ RIIA-mediated disease, but also reduced the disease index significantly below what was observed in nontransgenic mice, revealing an inhibitory signal that acts on other activating receptor pathways.

RA inflammation involves the release of cytokines (1) and ROS (27). In synovial fluid-infiltrating cells from RA patients, anti-hFc $\gamma$ RII F(ab)<sub>2</sub> targeting increased Syk recruitment to the receptor, which was rapidly followed by its disengagement and a stable recruitment of SHP-1. Activation of hFc $\gamma$ RIIA-ITAMi signaling on human monocytes and neutrophils resulted in the association of SHP-1 with major effectors (IRAK-1 and Vav-1) involved in cytokine and ROS production, respectively (38), thus allowing a pleiotropic inhibition of inflammatory cell activation.

The mechanism by which ITAM-bearing receptors mediate recruitment of SHP-1 was, however, unclear until now. Indeed, in previous studies using chimeric receptors made of the extracellular domains of hFc $\alpha$ RI or hFc $\gamma$ RIIIA and the intracellular domain of the Fc $\gamma$  subunit (hFc $\alpha$ RI-Fc $\gamma$  or hFc $\gamma$ RIIIA-Fc $\gamma$ , respectively), we failed to identify which tyrosine of the Fc $\gamma$  ITAM was implicated in the inhibitory signal (21, 24). The present study using hFc $\gamma$ RIIA mutants allowed us to identify differential structural requirements between ITAMa and ITAMi signaling. Whereas ITAMa signaling required phosphorylation of both tyrosine residues of ITAM, ITAMi signaling required only the membrane-distal tyrosine (Y304). Interestingly, phosphorylation of the 2 Fc $\gamma$  ITAM tyrosines is required for stable association and full activation of Syk, whereas a monophosphorylated Fc $\gamma$  ITAM allows only minimal association and activation of Syk (39, 40). In the light of these reports and based on our present findings, we suggest that hFc $\gamma$ RIIA ITAMi signaling starts with monophosphorylation of its ITAM, allowing a transient recruitment and minimal activation of Syk. This would permit phosphorylation and activation of SHP-1, followed by SHP-1 recruitment to the phosphotyrosine Y304 of the monophosphorylated ITAM, which remained accessible after Syk disengagement from

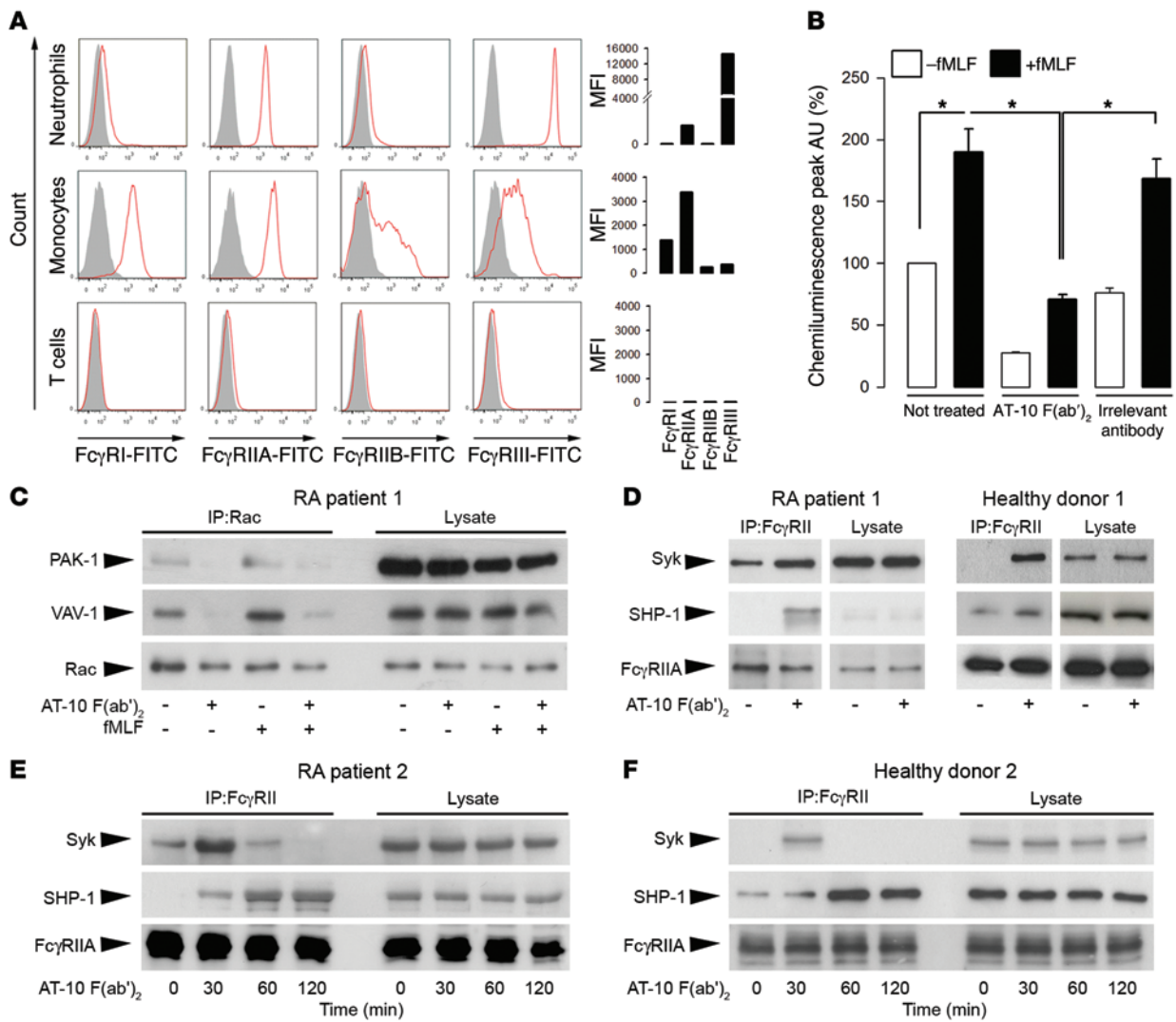


**Figure 9. hFcγRIIA ITAMi signaling inhibits ROS production, reversing inflammatory profile in synovial fluid-infiltrating cells from RA patients. (A)** Representative FcγR expression on infiltrating cells from RA patient as in Figure 7A. **(B)** Infiltrating cells isolated from the synovial fluid of RA patients were preincubated or not with AT-10 F(ab')<sub>2</sub> (10 μg/ml) for 30 minutes at 37°C before cell activation with or without fMLF for 30 minutes. Peak of ROS production was measured by luminol-amplified chemiluminescence 1 minute after stimulation. **(C)** Activated cells from **B** were lysed, and lysates were subjected to anti-Rac immunoprecipitation. Eluted material was then subjected to immunoblot analysis for the presence of indicated proteins. Protein amounts were also analyzed in lysates by immunoblotting. **(D)** Immunoprecipitation of hFcγRIIA from RA synovial fluid-infiltrating cells (left panel) or from healthy donor blood cells (right panel) that had been treated or not by AT-10 F(ab')<sub>2</sub> (10 μg/ml) for 30 minutes. The eluted material was then subjected to immunoblotting analysis for the presence of indicated proteins. Cell lysates were also analyzed by immunoblotting. **(E and F)** Human leukocytes isolated from the synovial fluid of an RA patient **(E)** or from a healthy donor's blood **(F)** were preincubated or not with AT-10 F(ab')<sub>2</sub> (10 μg/ml) for 0.5 to 2 hours. Cell lysates were then subjected to anti-hFcγRII immunoprecipitation. The eluted material was analyzed by immunoblotting for the presence of Syk, SHP-1, and hFcγRIIA. \*P < 0.05. Data represent 1 of 3 independent experiments.

the receptor. This mechanism significantly differs from the classical ITAMa signaling, in which dual tyrosine phosphorylation of the hFcγRIIA ITAM leads to stable recruitment of Syk and to its robust activation (Figure 10). The extent of receptor aggregation could be the critical parameter that determines a bias toward ITAMa or ITAMi signaling. Indeed, dimerization of FcRIIA was required for ITAMi signaling, since no signal was generated by monovalent engagement of the receptor (AT-10 Fab alone; not shown), whereas extensive aggregation of the receptor led to ITAMa signaling. This is also supported by published observations that a proportion of FcγRIIA is constitutively present as a dimer on the cell surface (41) and that monomeric IgG may stabilize these dimers (42). Similar

observations were obtained for FcγRIIA in which 3G8 F(ab')<sub>2</sub>, but not Fab anti-FcγRIII, can induce ITAMi signaling (24).

Because mAb AT-10 binds to both hFcγRIIA and hFcγRIIB, one may argue that the use of AT-10 anti-hFcγRII F(ab')<sub>2</sub> on synovial fluid-infiltrating cells from RA patients may also engage inhibitory hFcγRIIB. If engaged, hFcγRIIB is nevertheless unlikely to account for the drastic downregulation of their inflammatory phenotype following AT-10 anti-hFcγRII F(ab')<sub>2</sub> treatment, as indeed, only 6% of the cells were found to express hFcγRIIB (monocytes). Knockdown of FcγRIIB by siRNA in blood monocytes had no effect on ROS production, and hFcγRIIB was not expressed by THP-1 cells or by human neutrophils (75% of synovium-infiltrating cells),

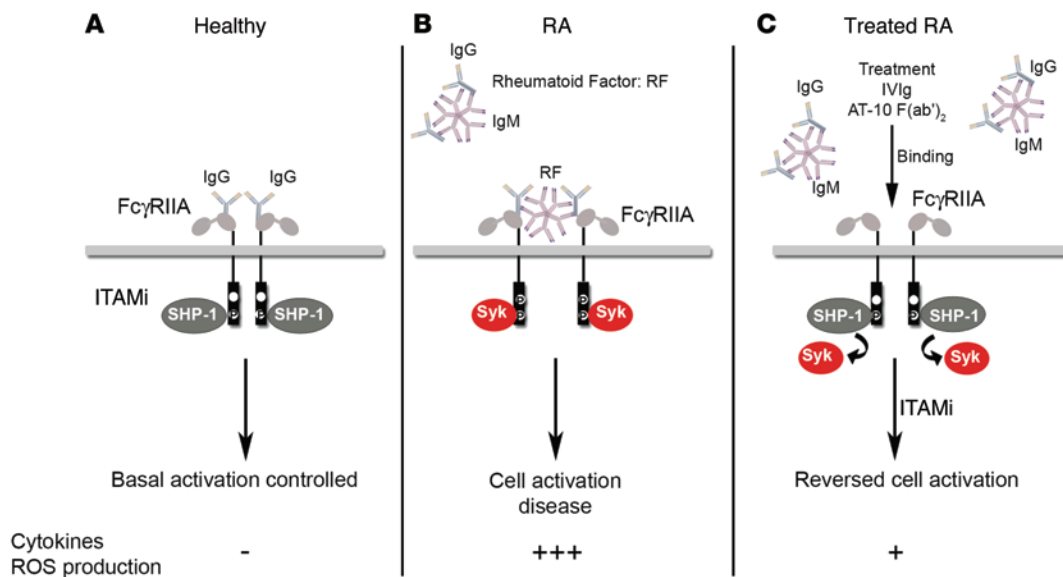


**Figure 10. Proposed model for anti-hFc $\gamma$ RIIA F(ab')<sub>2</sub> treatment in RA.** (A) In healthy individuals, hFc $\gamma$ RIIA exists in an ITAMi configuration with SHP-1 associated to its monophosphorylated ITAM as a possible result of hFc $\gamma$ RIIA binding by low-affinity natural autoantibodies or of hFc $\gamma$ RIIA inefficient triggering by monomeric circulating IgG. In this configuration, hFc $\gamma$ RIIA ITAMi maintains a low level of cell activation for optimal homeostasis. (B) In RA patients, the presence of circulating rheumatoid factors results in the binding of high-avidity ICs to hFc $\gamma$ RIIA, leading to stable aggregation of receptors, ITAMa signaling with stable recruitment of the kinase Syk to the doubly phosphorylated ITAM, cell activation, and production of inflammatory cytokines. This induces recruitment of additional inflammatory cells to the synovial cavity with further cell activation and production of ROS. (C) Treatment with anti-hFc $\gamma$ RIIA F(ab')<sub>2</sub> or with IVIg can displace ICs from hFc $\gamma$ RIIA and/or bind to free hFc $\gamma$ RIIA. In any case, this leads to restoration of an ITAMi configuration of hFc $\gamma$ RIIA with reversal of the inflammatory phenotype.

excluding involvement of this receptor in experiments performed with these cells. Supporting this conclusion, F(ab')<sub>2</sub> fragments of the hFc $\gamma$ RIIA-specific mAb IV.3 (which does not bind to hFc $\gamma$ RIIB) were sufficient to induce ITAMi signaling. These results together indicate that specific targeting of hFc $\gamma$ RIIA may constitute a promising approach for RA treatment.

While crosslinking of the receptor by ICs induces cell activation, IVIg or anti-hFc $\gamma$ RIIA F(ab')<sub>2</sub> fragments trigger a potent ITAMi signal, inhibiting various heterologous receptors. The ITAMi signaling had been previously demonstrated for Fc $\gamma$ R subunit-associated hFcRs, such as hFc $\alpha$ RI and hFc $\gamma$ RIIIA, or for DAP subunit-associated receptors, but not for a single-chain FcR such as hFc $\gamma$ RIIA (16). Our data demonstrate that an ITAM-containing single-chain receptor can also mediate efficient dual functions.

In summary, our study shows that hFc $\gamma$ RIIA can act and be used as a switch that controls the outcome of an inflammatory response. We report that one can swap the hFc $\gamma$ RIIA ITAMa signal observed in RA to an ITAMi signal reversing inflammatory responses. This opens new avenues for antibody-mediated antiinflammatory therapeutic approaches for RA based on hFc $\gamma$ RIIA targeting.

## Methods

**Subjects.** Synovial fluids from 7 patients with RA (without steroid and anti-CD20 treatments) were obtained during medical care. Blood from 10 healthy volunteers was collected.

**Mice.** Experiments were carried out on pathogen-free, 10- to 12-week-old female WT C57BL/6J, C57BL/6J hFc $\gamma$ RIIA-transgenic mice (15) and Fc $\gamma$ R<sup>-/-</sup> C57BL/6J mice obtained from the Jackson Laboratory. Fc $\gamma$ RIIA<sup>tg</sup>-Fc $\gamma$ R<sup>-/-</sup> mice were obtained as described previously (43). Nontransgenic littermates served as controls.

**Induction of arthritis.** Arthritis was induced following the method of Terato et al. (44) using an arthritogenic mAb cocktail. Mice were injected i.v. with 5 mg/20 g of mouse of anti-collagen II (anti-CII) Ab (Chondrex, GENTAUR) followed by an i.p. injection of 50  $\mu$ g LPS/20 g of mouse at day 3.

**Cells and reagents.** BMM from 6- to 8-week-old mice were obtained after a 7-day culture with CSF-1. RBL-2H3 cells expressing hFc $\gamma$ RIIA were maintained in DMEM supplemented with 10% FCS and 2  $\mu$ g/ml puromycin (Invitrogen). THP-1-Fc $\gamma$ RIIA-R131<sup>+</sup>-CD14<sup>+</sup> cell lines (provided by Novimmune) were maintained in RPMI-1640 supplemented with 10% FCS, 50  $\mu$ M  $\beta$ -mercaptoethanol, 200  $\mu$ g/ml Zeocin, 10  $\mu$ g/ml blasticidin, and 2  $\mu$ g/ml puromycin (Invitrogen). Human blood mononuclear cells were isolated by Ficoll-Hypaque density gradient centrifugation, and monocytes or neutrophils were purified by the Dynabeads Untouched Human Monocytes kit (Invitrogen) or by dextran sedimentation, respectively. Mouse anti-hFc $\gamma$ RII AT-10 mAb, which binds to an epitope located near or in the IgG-binding site (45), was purchased from Santa Cruz Biotechnology Inc. Mouse anti-hFc $\gamma$ RIIA IV.3 mAb, provided by C. Anderson (Department of Molecular Genetics, The Ohio State University, Columbus, Ohio, USA) (46, 47), was purified in house. AT-10, IV.3, and irrelevant control mAb (clone 320) were used as F(ab')<sub>2</sub>, prepared as previously described (21, 48). IVIg (Privigen; 100 mg/ml) was purchased from CSL Behring GmbH.

**Cytokine measurements.** After centrifugation (14,000 g, 10 minutes), THP-1-hFc $\gamma$ RIIA-R131<sup>+</sup>-CD14<sup>+</sup> cells or blood monocyte supernatants were kept at -80°C until measurement. The presence of MCP-1, TNF- $\alpha$ , IL-6, and IL-8/MIP-2 in the supernatants was determined using ELISA kits (R&D Systems) according to the manufacturer's instructions.

**Immunoprecipitation and immunoblotting.** Cells were solubilized in 1% digitonin-containing lysis buffer, and hFcγRIIA cells were immunoprecipitated over 2 hours at 4°C with either protein G or AT-10 F(ab)<sub>2</sub> coupled to CNBr-activated sepharose 4B (Amersham Pharmacia). Proteins were resolved by sodium dodecylsulfate–10% polyacrylamide gel electrophoresis, transferred onto nitrocellulose membranes (Invitrogen), and immunoblotted with primary antibodies such as rabbit anti-SHP-1 (Santa Cruz Biotechnology Inc.), anti-Syk (Santa Cruz Biotechnology Inc.), anti-Vav-1 (Cell Signaling Technology), anti-PAK1 (Cell Signaling Technology), anti-Rac (Santa Cruz Biotechnology Inc.), and anti-phospho-SHP-1 (ECM Biosciences) followed by goat anti-rabbit IgG (Jackson ImmunoResearch Laboratories) coupled to horseradish peroxidase (HRP). Membranes were developed by enhanced chemiluminescence (ECL) treatment (Amersham Biosciences).

**ROS measurement.** Human monocytes or neutrophils ( $5 \times 10^5$ ) were resuspended in 0.5 ml HBSS containing 10M luminol (Sigma-Aldrich) with AT-10 F(ab)<sub>2</sub> at 10 μg/ml or irrelevant 320 F(ab)<sub>2</sub> at 10 μg/ml for 30 minutes. Cells were stimulated with 1 μM fMLF (Sigma-Aldrich). Chemiluminescence was recorded with a luminometer (Berthold-Biolumat LB937). For BMM, cells were plated on Lab-Tek chambered coverglass slides (Nalge Nunc International), loaded with 50 μM DCFH-DA for 30 minutes, and stimulated with fMLF. After excitation at 488 nm, the green fluorescence of DCF was measured by confocal laser scanning microscopy (CLSM) (510-META, Carl Zeiss) equipped with a cell culture chamber at 37°C with a 5% CO<sub>2</sub> atmosphere.

**cDNA constructs, transfection, RT-PCR, siRNA, degranulation, and chemotaxis assays.** Details are described in Supplemental Methods.

**Flow cytometry, histopathology, and immunohistochemistry.** See Supplemental Methods for details, including antibodies used.

**Statistics.** Data analysis was performed using GraphPad Prism 5 software (GraphPad Software). Data are presented as the means ± SEM of at least 3 independent experiments. Comparisons were made by 2-tailed Student's *t* test for independent samples. A *P* value of less than 0.05 was considered statistically significant.

**Study approval.** Patients gave written informed consent before participating in this study and were enrolled in the study after approval by the Hôpital Bichat Claude Bernard ethical committee. Data collection and analyses were performed anonymously. All animal protocols were approved by the French Agricultural Office and by an INSERM ethical committee.

## Acknowledgments

The authors thank S. Benadda for confocal analyses; J. Bex-Coudrat, N. Ialy-Radio and A. Bouhafaia for animal care; and N. Quellard and B. Fernandez for histology. This work was supported by grants from Agence Nationale de la Recherche (ANR grants MIEN-2009 and BLANC International-2012) and by LabEx Inflammex. S.B. Mkaddem was supported by a grant from the French Foundation ARC (PDF20100601037).

Address correspondence to: Renato Monteiro, INSERM UMR 1149, Faculté de Médecine Paris Diderot – Site Xavier Bichat – 16, Rue Henri Huchard, Paris 75018 Cedex 18, France. Phone: 33.1.5727.7755; E-mail: renato.monteiro@inserm.fr.

- Nigrovic PA, et al. Mast cells contribute to initiation of autoantibody-mediated arthritis via IL-1. *Proc Natl Acad Sci U S A*. 2007;104(7):2325–2330.
- Boillard E, et al. Platelets amplify inflammation in arthritis via collagen-dependent microparticle production. *Science*. 2010;327(5965):580–583.
- Nigrovic PA, White PH. Care of the adult with juvenile rheumatoid arthritis. *Arthritis Rheum*. 2006;55(2):208–216.
- Monach PA, Mathis D, Benoist C. The K/BxN arthritis model. *Curr Protoc Immunol*. 2008;Chapter 15:Unit 15.22.
- Bruhns P. Properties of mouse and human IgG receptors and their contribution to disease models. *Blood*. 2012;119(24):5640–5649.
- Daeron M. Fc receptor biology. *Annu Rev Immunol*. 1997;15:203–234.
- Van den Herik-Oudijk IE, Ter Bekke MW, Tempelman MJ, Capel PJ, Van de Winkel JG. Functional differences between two Fc receptor ITAM signaling motifs. *Blood*. 1995;86(9):3302–3307.
- Dai X, et al. Differential signal transduction, membrane trafficking, and immune effector functions mediated by FcγRI versus FcγRIIA. *Blood*. 2009;114(2):318–327.
- Bruhns P, et al. Specificity and affinity of human Fcγ receptors and their polymorphic variants for human IgG subclasses. *Blood*. 2009;113(16):3716–3725.
- Jonsson F, et al. Mouse and human neutrophils induce anaphylaxis. *J Clin Invest*. 2011;121(4):1484–1496.
- Garcia-Garcia E, Nieto-Castaneda G, Ruiz-Saldana M, Mora N, Rosales C. FcγRIIA and FcγRIIB mediate nuclear factor activation through separate signaling pathways in human neutrophils. *J Immunol*. 2009;182(8):4547–4556.
- Parren PW, et al. On the interaction of IgG subclasses with the low affinity FcγRIa (CD32) on human monocytes, neutrophils, and platelets. Analysis of a functional polymorphism to human IgG2. *J Clin Invest*. 1992;90(4):1537–1546.
- Morgan AW, et al. Fcγ receptor type IIIA is associated with rheumatoid arthritis in two distinct ethnic groups. *Arthritis Rheum*. 2000;43(10):2328–2334.
- Tsuboi N, Asano K, Lauterbach M, Mayadas TN. Human neutrophil Fcγ receptors initiate and play specialized nonredundant roles in antibody-mediated inflammatory diseases. *Immunity*. 2008;28(6):833–846.
- Tan Sardjono C, et al. Development of spontaneous multisystem autoimmune disease and hypersensitivity to antibody-induced inflammation in Fcγ receptor IIA-transgenic mice. *Arthritis Rheum*. 2005;52(10):3220–3229.
- Smith KG, Clatworthy MR. FcγRIIB in autoimmunity and infection: evolutionary and therapeutic implications. *Nat Rev Immunol*. 2010;10(5):328–343.
- Hamerman JA, Lanier LL. Inhibition of immune responses by ITAM-bearing receptors. *Sci STKE*. 2006;2006(320):re1.
- Blank U, Launay P, Benhamou M, Monteiro RC. Inhibitory ITAMs as novel regulators of immunity. *Immunol Rev*. 2009;232(1):59–71.
- Ivashkiv LB. Cross-regulation of signaling by ITAM-associated receptors. *Nat Immunol*. 2009;10(4):340–347.
- Monteiro RC, Van De Winkel JG. IgA Fc receptors. *Annu Rev Immunol*. 2003;21:177–204.
- Pasquier B, et al. Identification of FcαRI as an inhibitory receptor that controls inflammation: dual role of Fcγ ITAM. *Immunity*. 2005;22(1):31–42.
- Kanamaru Y, et al. Inhibitory ITAM signaling by FcαRI-FcR gamma chain controls multiple activating responses and prevents renal inflammation. *J Immunol*. 2008;180(4):2669–2678.
- Pfirsch-Maisonnas S, et al. Inhibitory ITAM signaling traps activating receptors with the phosphatase SHP-1 to form polarized “inhibisome” clusters. *Sci Signal*. 2011;4(169):ra24.
- Aloulou M, et al. IgG1 and IVIg induce inhibitory ITAM signaling through FcγRIII controlling inflammatory responses. *Blood*. 2012;119(13):3084–3096.
- Clavel C, et al. Induction of macrophage secretion of tumor necrosis factor alpha through Fcγ receptor IIA engagement by rheumatoid arthritis-specific autoantibodies to citrullinated proteins complexed with fibrinogen. *Arthritis Rheum*. 2008;58(3):678–688.
- Dunn-Siegrist I, et al. Pivotal involvement of Fcγ receptor IIA in the neutralization of lipopolysaccharide signaling via a potent novel anti-TLR4 monoclonal antibody 15C1. *J Biol Chem*. 2007;282(48):34817–34827.
- McInnes IB, Schett G. Cytokines in the pathogenesis of rheumatoid arthritis. *Nat Rev Immunol*. 2007;7(6):429–442.
- Lawson CD, Donald S, Anderson KE, Patton DT,



- Welch HC. P-Rex1 and Vav1 cooperate in the regulation of formyl-methionyl-leucyl-phenylalanine-dependent neutrophil responses. *J Immunol.* 2011;186(3):1467-1476.
29. Han J, et al. Role of substrates and products of PI 3-kinase in regulating activation of Rac-related guanosine triphosphatases by Vav. *Science.* 1998;279(5350):558-560.
30. Stebbins CC, Watzl C, Billadeau DD, Leibson PJ, Burshtyn DN, Long EO. Vav1 dephosphorylation by the tyrosine phosphatase SHP-1 as a mechanism for inhibition of cellular cytotoxicity. *Mol Cell Biol.* 2003;23(17):6291-6299.
31. Kimura T, Zhang J, Sagawa K, Sakaguchi K, Appella E, Siraganian RP. Syk-independent tyrosine phosphorylation and association of the protein tyrosine phosphatases SHP-1 and SHP-2 with the high affinity IgE receptor. *J Immunol.* 1997;159(9):4426-4434.
32. Ganesan LP, Fang H, Marsh CB, Tridandapani S. The protein-tyrosine phosphatase SHP-1 associates with the phosphorylated immunoreceptor tyrosine-based activation motif of FcγRIIa to modulate signaling events in myeloid cells. *J Biol Chem.* 2003;278(37):35710-35717.
33. Pietersz GA, et al. Inhibition of destructive autoimmune arthritis in FcγRIIa transgenic mice by small chemical entities. *Immunol Cell Biol.* 2009;87(1):3-12.
34. Clark MR, Stuart SG, Kimberly RP, Ory PA, Goldstein IM. A single amino acid distinguishes the high-responder from the low-responder form of Fc receptor II on human monocytes. *Eur J Immunol.* 1991;21(8):1911-1916.
35. Monach PA, et al. Neutrophils in a mouse model of autoantibody-mediated arthritis: critical producers of Fc receptor γ, the receptor for C5a, and lymphocyte function-associated antigen 1. *Arthritis Rheum.* 2010;62(3):753-764.
36. Ji H, et al. Arthritis critically dependent on innate immune system players. *Immunity.* 2002;16(2):157-168.
37. Van de Velde NC, Mottram PL, Powell MS, Lim B, Holmdahl R, Hogarth PM. Transgenic mice expressing human FcγRIIa have enhanced sensitivity to induced autoimmune arthritis as well as elevated Th17 cells. *Immunol Lett.* 2010;130(1-2):82-88.
38. An H, et al. Phosphatase SHP-1 promotes TLR- and RIG-I-activated production of type I interferon by inhibiting the kinase IRAK1. *Nat Immunol.* 2008;9(5):542-550.
39. Kimura T, Kihara H, Bhattacharyya S, Sakamoto H, Appella E, Siraganian RP. Downstream signaling molecules bind to different phosphorylated immunoreceptor tyrosine-based activation motif (ITAM) peptides of the high affinity IgE receptor. *J Biol Chem.* 1996;271(44):27962-27968.
40. Kimura T, Sakamoto H, Appella E, Siraganian RP. Conformational changes induced in the protein tyrosine kinase p72syk by tyrosine phosphorylation or by binding of phosphorylated immunoreceptor tyrosine-based activation motif peptides. *Mol Cell Biol.* 1996;16(4):1471-1478.
41. Powell MS, et al. Alteration of the FcγRIIa dimer interface affects receptor signaling but not ligand binding. *J Immunol.* 2006;176(12):7489-7494.
42. Ramsland PA, et al. Structural basis for FcγRIIa recognition of human IgG and formation of inflammatory signaling complexes. *J Immunol.* 2011;187(6):3208-3217.
43. Jonsson F, et al. Human FcγRIIa induces anaphylactic and allergic reactions. *Blood.* 2012;119(11):2533-2544.
44. Terato K, et al. Collagen-induced arthritis in mice: synergistic effect of *E. coli* lipopolysaccharide bypasses epitope specificity in the induction of arthritis with monoclonal antibodies to type II collagen. *Autoimmunity.* 1995;22(3):137-147.
45. Greenman J, Tutt AL, George AJ, Pulford KA, Stevenson GT, Glennie MJ. Characterization of a new monoclonal anti-Fc γ RII antibody, AT10, and its incorporation into a bispecific F(ab')<sub>2</sub> derivative for recruitment of cytotoxic effectors. *Mol Immunol.* 1991;28(11):1243-1254.
46. Looney RJ, Abraham GN, Anderson CL. Human monocytes and U937 cells bear two distinct Fc receptors for IgG. *J Immunol.* 1986;136(5):1641-1647.
47. Astier A, et al. Detection and quantification of secreted soluble Fc gamma RIIa in human sera by an enzyme-linked immunosorbent assay. *J Immunol Methods.* 1993;166(1):1-10.
48. Fleit HB, Wright SD, Unkeless JC. Human neutrophil Fc γ receptor distribution and structure. *Proc Natl Acad Sci U S A.* 1982;79(10):3275-3279.